TO STUDY THE PERFORMANCE OF NANO-REFRIGERANT ($R134a+Al_2O_3$) BASED REFRIGERATION SYSTEM

Submitted in partial fulfillment of the requirement for the award of the degree

of

MASTER OF ENGINEERING

in

THERMAL ENGINEERING

Submitted By

Kuljeet Singh

Roll No. 801283014

Under the Guidance of

Mr. Kundan Lal

Assistant Professor

Department of Mechanical Engineering

Thapar University, Patiala

DEPARTMENT OF MECHANICAL ENGINEERING

THAPAR UNIVERSITY

(Established under section 3 of UGC Act, 1956 vide notification # F-12/84-U.3 of Government of India)

PATIALA-147004, INDIA

JULY - 2014

DECLARATION

I hereby declare that the thesis report entitled **"TO STUDY THE PERFORMANCE OF NANO-REFRIGERANT (R134a+Al_2O_3) BASED REFRIGERATION SYSTEM"** in the partial fulfillment of the requirements for award of the degree of **Master of Engineering in Thermal Engineering** submitted in **Department of Mechanical Engineering, Thapar University, Patiala,** is a record of work carried out under the supervision and guidance of **Mr. Kundan Lal, Assistant Professor, Department of Mechanical Engineering, Thapar University, Patiala.**

Place: 17/07/2014, PATIALA
Date:

Kuljeet Singh

This is to certify that above declaration made by the student concerned is correct to the best of my knowledge & belief.

Mr. Kundan Lal
Assistant professor
Thapar University,
Patiala - 147004

Countersigned by:

Dr.Ajay Batish
Professor & Head
Mechanical Engineering Department,
Thapar University,
Patiala - 147004

Dr. S.K. Mohapatra
Dean
Academic Affairs
Thapar university,
Patiala - 147004

ACKNOWLEDGEMENT

I would like to express a deep sense of gratitude and thank profusely to my guide **Mr. Kundan Lal** for his sincere & invaluable guidance, suggestions and attitude, which inspired me to submit seminar report in the present form. His dynamism and diligent enthusiasm have been highly instrumental in keeping my spirits high. His flawless and forthright suggestions blended with an innate intelligent application have crowned my task with success.

I am also thankful to **Dr. Ajay Batish,** Professor and Head, Department of Mechanical Engineering for his encouragement and inspiration for execution of the thesis work. Further, I would also like to thank Mr. Charanjit Singh and Mechanical Engineering department staff for their cooperation.

Kuljeet Singh

ABSTRACT

An experimental investigation into the performance of a vapour compression refrigeration system using pure refrigerant (R134a) and nanorefrigerant (R134a+Al_2O_3) has been conducted at the Mechanical Engineering Department, Thapar University, Patiala. The experimental apparatus has been assembled for this purpose which is similar to 165 litre commercial domestic refrigerator. It has already been known that the performance of the refrigeration system depends upon the heat transfer characteristics of the refrigerant being used. Literature review shows that the heat transfer characteristics of refrigerant R134a are poor as far as its thermal performance is concerned. In order to improve the thermal performance of the conventional refrigerant, an attempt has been made by injecting the nanoparticles along with the refrigerant into the refrigeration system. Aluminium Oxide (Al_2O_3) nanoparticles of 20 nm diameter are used with two different weight fractions (0.5 and 1%) in base refrigerant R134a. Experiments have been conducted with two refrigerant volume flow rates (6.5 and 11 LPH), two evaporator heat fluxes (at 15 ºC and 30 ºC) and at two ambient temperatures (21 ºC and 28 ºC). Addition of Aluminium Oxide (Al_2O_3) nanoparticles into the refrigerant R134a is found to be effective and a significant improvement in the thermo physical properties and heat transfer characteristics of the refrigerant is observed which results improvements in the performance of the refrigeration system. It has been also found that the refrigerant temperature drop across the condenser and temperature gain across the evaporator is higher when nanoparticles based refrigerant is used. The coefficient of performance (COP) is also found to be improved for 0.5% weight fraction but reduces with high weight fractions (1%) of nanoparticles in refrigerant. Moreover the nanorefrigerant (R134a + Al_2O_3) increases the cooling capacity (time to achieve a desired temperature) of refrigeration system. The experimental studies indicate that the refrigeration system works well with

nanorefrigerant. Thus, using aluminium oxide nanoparticles along with refrigerant in refrigeration system is feasible and within the investigated limits it gives a significant improvement in performance of the system.

Keywords:

Aluminum oxide (Al_2O_3), nanoparticles, nanorefrigerant, heat transfer characteristics, cooling, coefficient of performance (COP), power consumption, capacity

CONTENTS

LIST OF FIGURES

LIST OF TABLES

NOMENCLATURE

COP	: Coefficient of performance
Nm	: Nanometer
CNT	: Carbon nanotubes
LPH	: Liter per hour
TEM	: Transmission Electron Microscope
SEM	: Scanning Electron Microscope
kW	: Kilowatt
EG	: Ethylene Glycol
POE	: Polyolester
Kpa	: Kilo Pascal
Gm	: Gram
PAG	: Polyalkylene glycol
CFD	: Computational fluid dynamics
^{o}C	: Temperature in degree Celsius
Wh	: Watt hour energy consumed
wt%	: Concentration by weight
vol%	: Concentration by volume
T_1	: Temperature at compressor outlet
T_2	: Temperature at condenser outlet
T_3	: Temperature at expansion valve outlet
T_4	: Temperature at evaporator outlet

CHAPTER - 1

INTRODUCTION

1.1 NANOFLUIDS

Nanofluid is a fluid containing nanometer-sized particles, called nanoparticles. The nanoparticles used in nanofluids are typically made of metals, oxides, carbides or carbon nanotubes. Water, ethylene glycol and oil are commonly used as base fluids [1]. Size of nanoparticles is commonly varies from 20 nm to 100 nm. The smallest nanoparticles of few nanometers of diameter may contain thousands of atoms. The properties that the nanoparticles can possess are significantly different from their parent materials and nano scaled particles may interact differently within their molecular bond with the base fluids than the microparticles and respond differently for mass and energy transfer applications. Nanofluids are basically belong to a two-phase systems, in which solid phase is dispersed in liquid phase. But, literature also shows that in many cases nanofluids are also considered as a single phase fluid. The thermo-physical properties such as thermal conductivity, convective heat transfer coefficients, thermal diffusivity and viscosity have been found improved in case of nanofluids as compared to base fluids like oil or water. This improvement in thermo-physical properties demonstrated great potential applications in many fields of engineering [2].

Advantages

(i) High specific surface area (SSA) and therefore, more heat transfer surface between particles and fluids

(ii) The suspended nanoparticles in base fluid results enhancement in thermal conductivity

(iii) Reduced pumping power to achieve an equivalent heat transfer intensification which results system minimization

(iv) Lesser energy requirements due to system minimization and improved heat transfer and heat carrying capacities

(v) Properties like thermal conductivity and surface wettability are made adjustable by varying particle concentrations in base fluid, to suit different applications

(vi) Particle clogging can be reduced as compared to conventional slurries, hence it promotes system miniaturization

1.2 NANOFLUID'S CHALENGES

There are some important issues which are needed to be addressed for this two-phase system. Stability of nanofluid is one of the major problems and it remains a big challenge to achieve desired stability of nanofluids. In addition to stability of nanofluids, other key issues which require attention are as follows:-

(i) Agglomeration - It is kind of cluster formation of nanoparticles after a period of time. It may be before or after the mixing in base fluid. Particles dispersed in base fluid may adhere together and form aggregates of increased size which may settle down due to gravity action. This agglomeration not only results settlement and clogging but thermal conductivity of nanofluid also decreased. When nanoparticles get agglomerated, they often lose their high-surface area due to grain growth. This also affects its heat transfer performance.

(ii) Viscosity enhancement - Addition of nanoparticles in base fluid also enhances the viscosity of mixture or nanofluid. Due to this pressure drop tends to increase in flow applications, and which demand more pumping power. So depending upon applications, quantity of nanoparticles should be optimized.

(iii) Abrasion and erosion - Due to high velocity of particles in pipe flow the effect of erosion will come into picture. This may result wear and tear of piping system.

(iv) Sedimentation - Settling down of particles due to high density. If particle size is large then it will settle down and properties of nanofluid will be affected.

1.3 STABILITY OF NANOFLUIDS

As already discussed, the agglomeration and clustering of nanoparticles in the nanofluid takes place before and after the nanofluid production and during its application. So depending upon the different factors following stability methods are commonly used:-

(i) Use of surfactants - These are also known as dispersants. Use of surfactants in the nanofluids is an easy and economical method to enhance the nanofluid stability. Surfactants basically affect the surface characteristics of a system. They consist of a hydrophobic tail portion which is usually a long-chain hydrocarbon and a hydrophilic polar head group. Dispersants are employed to increase the wettability between two phases. In a nanofluid, a surfactant tends to locate at the interface of the two phases, so basically it introduces a degree of continuity between the base fluid and nanoparticles. However for high temperature applications, the functionality of the surfactants is also a big concern. According to the composition, dispersants are classified into four classes: nonionic surfactants without charge groups (include alcohols, polyethylene oxide, and other polar groups), anionic surfactants with negatively charged head groups (include long-chain fatty acids, alkyl sulfates, sulfosuccinates, sulfonates and phosphates), cationic surfactants with positively charged head groups (include protonated long-chain amines and long-chain quaternary ammonium compounds), and amphoteric surfactants with zwitterionic head groups charge depends on pH (include betaines and certain lecithins) [3].

(ii) **Surface modification techniques (surfactant free method) -** Use of functionalized nanoparticles is a promising approach to achieve long-term stability of nanofluids, this technique represents the surfactant free approach. Some investigations show the work regarding the synthesis of functionalized Silica (SiO_2) nanoparticles by grafting silanes directly to nanoparticles surface in original nanoparticle solutions. By doing this a unique characteristics of the nanofluids was found that after a pool boiling process no deposition layer formed on the heated surface. Researchers have also introduced hydrophilic functional groups on the nanotubes surface by mechanochemical reactions. The prepared nanofluids have no contamination to medium, low viscosity, enhanced stability, good fluidity and high thermal conductivity and also have potential to be used as coolants in thermal systems. This chemical modification to functionalize the surface of carbon nanotubes is a common method which results more stability of carbon nanotubes in solvents. One other method is used to modify the surface characteristics of diamond nanoparticles is Plasma Treatment. Plasma treatment uses gas mixtures of methane and oxygen, various polar groups are imparted on the surface of the diamond nanoparticles, which improves their dispersion property in water [3].

(iii) **Ultrasonic vibration -** Use of ultrasonic bath, processor and homogenizer are very effective techniques to break down the agglomerations. Ultrasonic vibrations are used to separate the particles. In this method nanoparticles are separated with strong and irregular ultrasonic shock inside the interaction chamber. This helps to get homogeneous suspensions of nanoparticles in base fluid with fewer aggregated particles at high-pressure. This procedure can be repeated for number of times (generally three times) to achieve the required homogeneous distribution of particles in the base fluids. This is an effective and simple method to eliminate agglomeration [3].

(iv) Other stability mechanisms - The term stability refers that the particles do not aggregate at a notable rate. The rate of aggregation is determined by the collisions frequency and the cohesion probability of during collision. Derjaguin, Verway, Landau and Overbeek (DVLO) developed a theory to achieve colloidal stability [2]. DLVO theory propose that the particle stability in solution (nanofluid) is determined by the sum of attractive and electrical double layer repulsive forces of van der Waals, which exist between particles. If the force of attraction is greater than the force of repulsion, than two particles will collide, and the suspension is unstable. If a sufficient high repulsion is there between particles, the suspensions will be more stable. To have stable nanofluids, the repulsive forces between nanoparticles must be dominant. According to the types of repulsion, there are two fundamental mechanisms that affect solution stability, which are known as steric repulsion, and electrostatic repulsion. In steric stabilization, suspension system involves polymers and they will adsorb onto the nanoparticles surface, this results an additional steric repulsive force, which makes the nanofluid more stable. For example, if Zinc oxide (ZnO) nanoparticles can be modified by polymethacrylic acid (PMAA), this will result good compatibility with polar solvents. Silver nanofluids are found very stable when surface is modified with polyvinylpyrrolidone (PVP), which retards the growth and rate of agglomeration of nanoparticles will be reduced by steric effect. The Graphite suspension can also become more stable with the use of PVP. In electrostatic stabilization, to generate repulsive forces the surface charge will be developed on particles. It may be obtained through following mechanisms:-

(i) Preferential adsorption of ions

(ii) Dissociation of surface charged species

(iii) Accumulation or depletion of electrons at the surface

(iv) Physical adsorption of charged species onto the surface [2]

1.4 PREPARATION OF NANOFLUIDS

(i) Two-step method - This is most widely used method for preparing nanofluids. Nanoparticles, nanofibers, nanotubes or other nanomaterials are first produced as dry powders by some chemical or physical methods. After preparing nanosized powder, it will be dispersed in base fluid in the second step of processing. The dispersion is done with the help of intensive magnetic force agitation, ultrasonic agitation, high-shear mixing, homogenizing and ball milling. Two-step method is found most economical method to produce nanofluids in large scale. The nanopowder synthesis techniques have already been scaled up for industrial production. But solutions prepared by two-step method have less stability. So to overcome this difficulty several advanced techniques are developed to produce nanofluids which include one-step method also [2].

(ii) One-step method - One-step physical vapour condensation method which has been developed to prepare Cu/ethylene glycol nanofluids with reduced agglomeration of nanoparticles. This method consists of simultaneously making and dispersing the nanoparticles into the base fluid. So drying, storage, transportation and dispersion processes of nanoparticles can be eliminated, which results minimization of the agglomeration of nanoparticles, hence the stability of nanofluids can be improved. This process can produce uniformly dispersed nanoparticles and the particles can be suspended stably in the base fluid. The vacuum-submerged arc nanoparticle synthesis system (SANSS) is another effective method used to produce nanofluids using different dielectric liquids. The different morphologies of nanofluid are mainly affected and determined by various thermal physical properties of the dielectric liquids. The nanoparticles produced by this method mainly exhibit needle-like, polygonal, circular and square morphological shapes. The method also avoids the undesired particle aggregation to greater extent. But one-step physical method is not economical to synthesize nanofluids in large scale

and it costs high, due to this reason the one-step chemical method is rapidly developing. Zhu et al. introduced a novel one-step chemical method for producing copper nanofluids by reducing $CuSO_4.5H_2O$ with $NaH_2PO_2.H_2O$ in ethylene glycol base fluid under microwave irradiation. This method gives well-dispersed and more stable copper nanofluids. Mineral oil-based nanofluids with silver nanoparticles with a narrow size distribution were also prepared efficiently by this method. The silver nanoparticle suspensions were found stable for about 1 month. Stable ethanol based nanofluids with silver nanoparticles can be prepared by microwave-assisted one-step method. In this method, polyvinylpyrrolidone (PVP) was used as the stabilizer and reducing agent for silver nanoparticles in solution. The cationic surfactant octadecylamine (ODA) is also an effective agent for phase-transfer to synthesize silver solutions. However one-step method also have some disadvantages, in which the most important is that in this method the residual reactants are left in the nanofluids due to incomplete stabilization or reaction. It is difficult to have good nanofluid without eliminating this impurity effect [2].

(iii) Other methods - Yu et al. [2] devolved a microfluidic microreactor with continuous flow to produce copper nanofluids. This method, can synthesize copper nanofluids continuously. The properties and microstructure of nanofluids can also be varied by adjusting parameters such as flow rate, nanoparticle concentration and additives. CuO nanofluids with high volume concentration (up to 10 vol%) can be effectively produced through a novel precursor transformation method with the help of microwave and ultrasonic irradiation. The precursor $Cu(OH)_2$ is completely transformed into CuO nanoparticle in base fluid water under microwave irradiation. The ammonium citrate prevents the growth and agglomeration of nanoparticles, which results stable CuO water nanofluid with higher value of thermal conductivity than those prepared by other methods. Phase-transfer method is also a effective process to obtain monodisperse noble metal nanofluids. In a water-cyclohexane two-phase system, aqueous

formaldehyde has been transferred to cyclohexane phase with the help of reaction with dodecylamine to form reductive intermediates in cyclohexane. The intermediates are also capable of reducing silver or gold ions in aqueous solution to form dodecylamine protected gold and silver nanoparticles in cyclohexane solution at room temperature. Aqueous-organic phase-transfer method can be also used for preparing silver, gold and platinum nanoparticles as solubility of PVP in water decreases with the increase in temperature. Phase-transfer method is also applied to prepare stable kerosene based nanofluid having Fe_3O_4 nanoparticles. Fe_3O_4 nanoparticles are successfully grafted by oleic acid, this results good compatibility of Fe_3O_4 nanoparticles with kerosene. But the production of nanofluids with controllable microstructure is key issue. It is known that properties of nanofluids are strongly dependent on the structure and shape of nanoparticles. The recent research found that nanofluids prepared by chemical solution method have better stability and higher conductivity enhancement than those produced by the other methods [2].

1.5 APPLICATIONS OF NANOFLUIDS

(i) Heat Exchangers - One of the major challenges for that industries faced includes cooling. The general approach adopted to enhance cooling rate is increase in heat transfer area. At same time balance between heat transfer and pumping cost should also be there, because as the heat transfer area increased the energy required to circulate the fluid through the heat exchanger goes up. Moreover increased heat transfer area needs bigger thermal management system. To tackle this problem nanotechnology found energy-efficient solution. Researchers have already developed nanofluids with increased forced convective heat transfer, which is four times more than water [5]. When these made to work in boiler, the central heating device found 10% more efficiency. Future research work on the nanofluid cooled microchannel heat exchanger will result the

effective cooling of high heat load X-ray monochromators. With the use of nanofluids in the high aspect ratio microchannels, power densities of 3000W/cm^2 are achievable. Figure 1 shows the heat exchanger efficiency with different types of nanofluids [5].

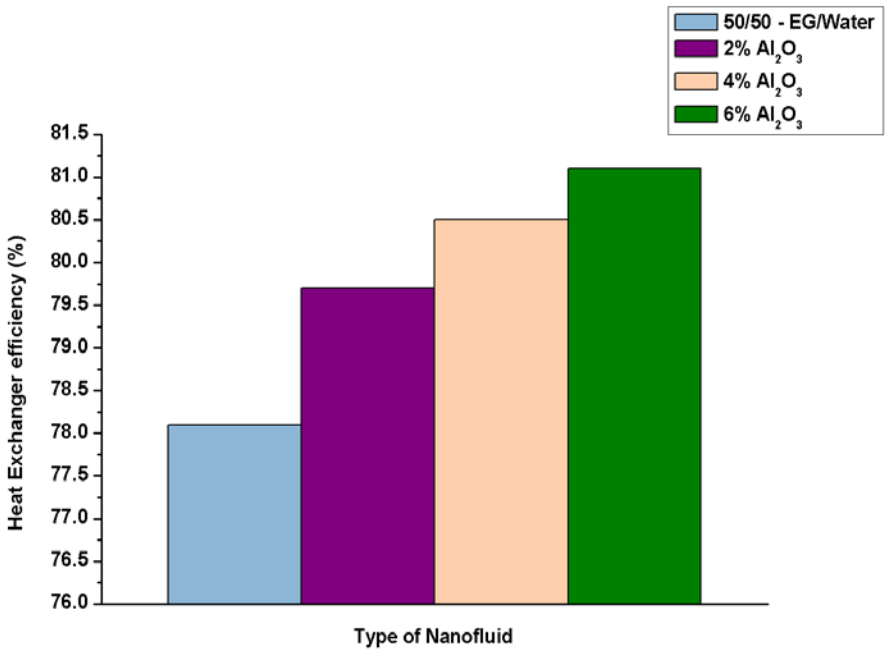

Figure 1.1 - Heat exchanger efficiency with nanofluids [5]

(ii) Engine cooling/vehicle thermal management - Vehicle thermal management is termed as more considerable because it directly or indirectly affects the performance of engine, fuel economy, safety, reliability, passenger comfort, selection of materials, emissions, component life and maintenance. So this demands an effective and responsive thermal management system to be designed for fuel-efficient operation that can meet increasingly stringent standards of emissions. The mixture of ethylene glycol and water is generally used as automotive coolant, which relatively have poor heat transfer rate compared to water alone. The standard engine coolant based nanofluids are found very effective to improve automotive engine cooling rates. Such improvement may also result minimization of coolant system to remove engine heat. Thus

smaller cooling systems will have smaller and lighter radiators, which give benefit in almost every aspect of car and economy [5].

(iii) Diesel combustion - Several studies are also conducted on addition of nanoparticles to fuels and propellants. These studies found multiple advantages of adding nanoparticles to solid fuels and propellants, which includes reduced ignition delay, improved energy density and high combustion rates. Some other studies have also shown improvement physical properties of fuel such as mass diffusivity, thermal conductivity and radiative heat transfer with the addition of nanoparticles. Moreover, some work has also been reported in the past, which showed the improvement in performance by adding nanoparticles to liquid fuels [5].

(iv) Boiler exhaust flue gas recovery - Utilization of the exhaust gases heat is an important and critical issue in boiler to minimize the losses. Hence operating economy is greatly dependent on it. Some research work has also been carried out in this area regarding the use of nanofluids and it is found that the heat of exhaust gases can be efficiently extracted by using nanofluids [4].

(v) Heating and cooling of buildings - Nanofluids can be also used in traditional heat exchangers which are used for heating and cooling of buildings. It has been found that application of nanofluid may result reduced volumetric flow rates, reduced mass flow rates and saving in pumping power. The use of nanofluids also needs smaller heating systems which are capable of deliver the same amount of thermal energy, thus system minimization can be achieved, thus lower initial cost of equipment. This will result reduced emission of pollutants into the atmosphere due to power consumption reduction and reduced waste produced at the end of the heat transfer system life-cycle. Moreover the nanofluids can be also in cooling systems instead of chilled water, which is generally used in cooling coils of air conditioning ducts [5].

(vi) Cooling of electronics - As international technology road map for semiconductors, the heat flux produced from a single chip is increased from 330W/cm^2 in 2007 to 520W/cm^2 in 2012 for high

performance chips. Hence, an effective cooling system is a critical hurdle in designing electronic components. Researchers have made several attempts to remove high heat flux effectively from an electronic system which includes liquid cooling, air cooling and two-phase cooling. So nanofluids can be used in this area to accelerate the cooling rate. In recent study it has been found that when liquids coolant with nanoparticles are exposed to electric fields it showed improved performance and stability, which may lead to new kind of miniature camera lenses, display of mobile phone and other micro scale fluidic devices. Following type of study opened up a new window for nanofluids use in nano scale and micro scale actuator device applications [2].

(vii) Application as a coolant in machining - In machining tool life is greatly dependent on heat liberated and friction that involved in cutting process. This is also considered as major challenge. To tackle this problem the conventional choice is cutting fluids. But its heat carrying capacity and potential of adequate lubrication is found to be limited. Hence in vista of the above hurdles, the nanofluids application has gained interest. The cooling and lubricating properties of nanofluids are found effective and hence this can be considered as a promising solution. The work has been reported regarding the improvement in the heat transfer characteristics of cutting fluids with the addition of nanoparticles (enhanced upto 6%) [5].

(viii) Nanofluids in transformer cooling oil - The oil used for cooling of transformers is serving the industry well but at same time the problems of cost of replacement, too much maintenance, environmental jeopardy and failure incidence due to overheating are there. Transformer oil is a very poor conductor of heat, hence localized hot spots results cracking of the oil's molecular composition and insulation collapse. Studies showed the addition of nanoparticles in transformer oil improves the overall thermal conductivity of oil [34].

(ix) Nuclear systems cooling - The nanofluids can be used in water-cooled nuclear systems which may lead to a significant improvement in economic performance and safety margins. It has found that the system has a reasonably low failure probability with the use of nanofluids. Analytically it has been revealed that use of nanofluids result increase in decay power removal through the vessel, which is around 40%, which may lead to achieve higher vessel retention safety margin and enable enhanced core power [5].

(x) Solar water heating - The work presented that shows that the improvement in thermal conductivity is greatly dependent on the volume fraction of added particles and thermal conductivities of base fluids and nanoparticles. Moreover the study also states that the nanofluid is more effective and efficient than conventional fluids. So water based nanofluids can also be used as heat transport medium in solar systems (solar water heaters). This increases the efficiency of the traditional solar water heaters and also results system minimization for same capacities [34].

(xi) Refrigeration (domestic refrigerator, chillers) - The work has been reported regarding nanofluid application in chillers which shows 40% enhancement in thermal conductivity with about 0.4% volume fraction of nanoparticles. This unveils the scope of application of nanofluids in chillers of air conditioning systems. It has been also found that the cooling capacity of the system can be improved by 4.2% at the standard conditions. Whereas with 60 L/min volume flow rate the increase of 6.7% in the capacity have been achieved. Moreover coefficient of performance (COP) at standard rating conditions has also been increased by 5.15%. In some other studies nanoparticles have been mixed with lubricating oil of compressor of domestic refrigerator, which also showed impressive results [5].

(xii) Application of nanofluids in thermal absorption systems - This is a serious topic of discussion that vapour compression system lead certain environmental problems such as

depletion of ozone layer and global warming due to use of refrigerants. Vapour absorption system is an alternative to the vapor compression system as it is driven thermally. Most critical component of an absorption system is absorber. Hence several experimental studies have been conducted to improve the performance of the absorber by using nanoparticles. Study revealed that addition of Al_2O_3, CuO and Cu nanoparticles in a NH_3-H_2O base fluid enhanced the performance absorption by 5.32 times [5].

(xiii) Application in oscillating heat pipes - Researchers have also unveiled that the use nanofluids in oscillating heat pipes (OHP) considerably increases the heat carrying capacities. In order to find out the primary factors that affecting the heat transfer improvement of the OHP, the thermal conductivity of the motionless nanofluids was measured. The results of this study showed that the diamond nanoparticles can improve the thermal conductivity of nanofluids. The nanofluid's thermal conductivity was found to be 1.0W/mK whereas the thermal conductivity of HPLC grade water was in order of 0.6W/mK at 21^{o}C ambient temperature. So these results show that nanofluid can enhance the thermal conductivity, which lead to increase in heat carrying capacity of the oscillating heat pipes OHP [34].

(xiv) Defense - Military devices and systems requires high heat flux cooling which can be in level of tens of MW/m^2. So to achieve that much of cooling the use of conventional fluids is found challenging. Military applications may involve power electronics and directed energy weapons cooling. In case of directed energy weapons the heat fluxes are as high as 500–1000W/cm^2 and to provide cooling at sufficient rate is a critical issue. In same manner the heat associated with power electronics is also need to be extracted to ensure effective operation. Nanofluids have that potential by which adequate cooling in such applications can be achieved. In addition to this other military systems such as vehicles, submarines and high-power laser diodes can be operated at optimize level with the help of nanofluids [2].

(xv) Space - Cooling of satellite is also a big challenge and this issue is critical also due to high costs of satellites. Nanofluid can be an efficient coolant alternative in space applications.

(xvi) Biomedical applications - It has also been found that nanoparticles and nanofluids can be used in the biomedical industry, but some side effects are also involved in traditional methods of cancer treatment. Some studies also revealed the use of Iron based nanoparticles as delivery vehicles for drugs or radiation without damaging nearby healthy tissue. Through blood stream these nanoparticles could be guided to a tumor using external magnets to the body. Nanofluids could also be used to produce effective cooling around the surgical region for safer surgeries, which lead to increase in survival chance of patient and reducing the organ damage threat. Bio-fluids having magnetic particles could be used as delivery vehicles for drugs or radiation in new cancer treatment methods [5].

(xvii) An application in fuel cells - Fuel cell is new advancement in the power generation sector. Operation of fuel cell includes notable amounts of heat and mass exchange. Whenever the heat transfer process occurs within the fuel cell or in its auxiliary heat recovery systems, the application of nanofluids is come into picture and it can be employed to improve heat exchange and increase the efficiency of fuel [5].

1.6 REFRIGERATION SYSTEMS AND NANOFLUIDS

The application of nanofluids in refrigeration system is also found effective in order to improve its performance. The application of nanoparticles in refrigeration systems is a point of attraction because of its outstanding capability to improve thermophysical properties, heat carrying capacities and heat transfer capabilities. These improvements can play a key role to enhance the performance of refrigeration systems. Recently, some studies have been carried out on vapour compression refrigeration systems to investigate the effect of nanoparticles (added to lubricant or

refrigerant) on performance of the system. In a vapour compression refrigeration systems the nanoparticles can be added to the lubricating oil of compressor. During refrigeration cycle, when the refrigerant is circulated through the compressor it carry lubricant + nanoparticles mixture (nanolubricant). So, by this way other parts of the refrigeration system will have nanolubricant-refrigerant mixture, which results in improved heat transfer rates in condenser and evaporator. Nanoparticles added in lubricating oils may also lead to decrease in coefficient of friction and wear rate. It has also been found that dispersion of nanoparticles lead to considerable increase in the critical heat flux. Some experimental studies have shown that there is notable diminution in the power consumption and considerable enhancement in freezing capacity. These remarkable improvements in performance of the system are due to enhanced thermo physical properties of nanolubricant. When nanoparticles are added to base refrigerant the mixture is called nanorefrigerant. Some studies have been reported on R123, R141b and R600a based nanorefrigerants which show the improvement in the performance of the system. So, this all capture researcher's attention and demands further work to explore the nanofluids application in refrigeration and air conditioning filed in order to improve its performance and system minimization.

CHAPTER - 2

LITERATURE SURVEY

The literature review on nanofluid applications in refrigeration systems, gaps in study and objectives for the proposed work have been presented in this chapter. In refrigeration systems the nanoparticles are used in two ways either by dispersing it in compressor lubrication oil (nanolubricant) or mixing with refrigerant (nanorefrigerant). Literatures regarding improvement in heat transfer coefficients, boiling heat transfer characteristics, coefficient of performance (COP), reduction in power consumption and system minimization have been discussed in detail.

2.1 LITERATURE REVIEW

Park et al. [6] conducted a study to evaluate effect on heat transfer coefficient for nanofluid based refrigerant during pool boiling. For this purpose different refrigerant (R22, R123 and R134) and carbon nanotubes were used. Three types of nanofluid samples were prepared for this purpose, listed as R22 + CNT, R123 + CNT and R134a + CNT. In this investigation it was found that in horizontal smooth tube CNTs improved the pool boiling heat transfer coefficients of base fluid (refrigerants). It had been also reported that the improvement became more prominent at lower value of heat flux and the maximum improvement of 36.6% could be reached. Hence use of CNTs in refrigerants was found to be effective in order to enhance heat transfer coefficient.

Trisaksri et al. [7] carried out an experiment to study the behavior of nanorefrigerant during nucleate pool boiling. In this study R141b is used as base refrigerant with TiO_2 nanoparticles and a horizontal cylinder of copper of 28.5 mm diameter was used for boiling. It was found out that

adding a small quantity of nanoparticles to refrigerant R141b did not affect on boiling heat transfer rate, but when dispersion of TiO_2 nanoparticles is increased from 0.03% to 0.05% (vol.), it reduces the boiling heat transfer rate. In addition to this, at higher heat flux the boiling heat transfer coefficient was found to be decreasing with increase in particle volume concentrations.

Hao et al. [8] carried out an investigation to study the heat transfer coefficient of nanorefrigerant during flow boiling through a smooth tube. Following study was conducted with different nanoparticles concentration, heat fluxes, mass flow rates and inlet vapour qualities and the effect of nanoparticles on the heat transfer coefficient was analyzed. Investigation taken refrigerant R113a as base fluid and CuO of 40 nm diameter size was used as nanoparticles material. Mass fractions of nanoparticles in refrigerant were taken as 0.1%, 0.2% and 0.5%. An ultrasonic vibration was used to stabilize the nanoparticles suspension in nanofluid. No surfactant was added to mixture as it may affect the heat transfer properties. The maximum enhancement in heat transfer coefficient was found to be 29.7% during flow boiling.

Hao et al. [9] carried out an experimental study to evaluate heat transfer characteristics of refrigerant/oil with dispersed diamond nanoparticles during nucleate pool boiling. In this study R113 was taken as refrigerant, whereas VG68 was used as lubricating oil. Experiment was conducted at saturation pressure of 101.3 kPa. Heat flux had been varied from 10 to 80 kW/m^2, whereas concentrations of nanoparticles in the oil was varied from 0 to 15% by weight and nanoparticles + oil dispersion in refrigerant was varied from 0 to 5% by weight. The results showed that during nucleate pool boiling the heat transfer coefficient of R113 + oil + diamond nanoparticles was found to be greater than R113 + oil mixture by maximum of 63.4% under the above conditions. The improvement was found increasing with increase in concentration of

nanoparticles in the oil and decreases with the increase in nanoparticles + oil concentrations in refrigerant R113.

Coumaressin et al. [10] conducted an experiment in which effect of R134a based CuO nanofluid on evaporating heat transfer coefficient was evaluated with the help of CFD heat transfer analysis through FLUENT. Heat flux was varied from 10 to 40 kW/m^2, particle size (CuO) from 10 to 70 nm and concentration from 0.05% to 1%. In this study it was found that by using CuO nanoparticles in combination with R134a evaporating heat transfer coefficient increases upto 0.55% concentration and then decreases, this trend was followed with all heat fluxes. At 0.55% concentration heat transfer coefficient of evaporation was found to be highest for all values of heat fluxes.

Kedzierski et al. [11] carried out an investigation to study the boiling performance of R134a/ polyolester based nanofluid with CuO nanoparticles of 30 nm diameter. The behavior was studied by boiling the mixtures on a horizontal flat rough surface. 1% volume fraction of CuO in polyolester lubricant was added and the same was used with R134a at three different mass fractions. Studies concluded that for 0.5% mass fraction of nanolubricant with R134a heat transfer coefficient improves from 50% to 275% compared to heat transfer coefficient for pure R134a/polyolester (99.5/0.5). Whereas less improvement was found with 1% mass fraction of nanolubricant in R134a, which was around 19% more than pure R134a/ polyolester (99/1) mixture. Further nanolubricant with 2% mass fraction resulted heat transfer improvement in order of 12% as compared to R134a/polyolester (98/2) mixture. So the investigation concluded that the improvement in performance with nanolubricant decreases with increase in nanolubricant concentration in R134a.

Bi et al. [12] carried out an experimental study on domestic refrigerator using nanoparticles in the working fluid and reliability and performance of was investigated. Mineral oil was used as lubricant instead of Polyol-ester (POE) and R134a (1,1,1,2-tetrafluoroethane) was taken as refrigerant. TiO_2 nanoparticles were dispersed in mineral oil. After conducting compatibility study, the performance of domestic refrigerator with nanolubricat was investigated with the help of energy consumption and freeze capacity tests. In this study it had been found that R134a and nanolubricant (mineral oil+TiO_2 nanoparticles) worked normally in the refrigerator. The performance of refrigeration system was found better than the R134a + POE oil system, with 26.1% reduction in energy consumption when 0.1% mass fraction of TiO_2 nanoparticles was dispersed in mineral oil. Nanoparticles also increased the solubility of R134a and mineral oil. Thus use of nanoparticles in domestic refrigerators was found useful to reduce energy consumption.

Jwo et al. [13] conducted an experimental study on a vapour compression refrigeration system in which refrigerant R-134a and polyester lubricating oil had been replaced with a hydrocarbon refrigerant and mineral oil lubricant. Al_2O_3 nanoparticles ware dispersed in mineral lubricant to improve the heat-transfer characteristics and lubrication properties. In this study 60 gm R-134a and 0.1 wt % Al_2O_3 nanoparticles were found optimal. With above conditions, there was 2.4% reduction in power consumption and the coefficient of performance (COP) was increased by 4.4%.

Subramani et al. [14] done experimental study on a test rig consists of a compressor (hermetically sealed), air-cooled condenser (forced convection), thermostatic expansion valve and an evaporator. Evaporator was immersed in water. Al_2O_3 nanoparticles with average size

<50nm were dispersed in lubricating oil (SUNISO 3GS – a mineral oil) by two step method. 0.06% mass fraction of nanoparticles in the nanoparticle–lubricant mixture and it made stable with an ultrasonic vibrator. Dispersion of Al_2O_3 nanoparticles found stable for 3 days without coagulation or deposition. R134a was used as refrigerant. Three types of lubricant (filled in hermetic compressor) samples named as pure POE oil, SUNISO 3GS oil (mineral oil) and SUNISO 3GS+ Al_2O_3 nanoparticles were used in this study.. The condenser pressure was kept at 1.2 MPa and the evaporator pressure was 0.2 MPa. It was observed in this investigation that time required to bring the cooling load temperature from 28^{o}C to 5^{o}C was less in case of mineral oil + Al_2O_3 as compared to other samples. Mineral oil based nanoparticles sample took about 16.7% and 28.6% less time than pure mineral oil and POE oil samples respectively. Freezing capacity also found improved, the time taken to reduce the temperature of the cooling load from 28^{o}C to 1^{o}C with POE oil was 110 minutes and it reduces by 27 % if mineral oil + Al_2O_3 sample used. Subcooling was also achieved in condenser with the use of nanolubricant. Power consumption of the compressor was also found to be decreased by 25% with nanolubricant as compared to POE oil. Moreover the coefficient of performance (COP) of system was also found higher in case of nanolubricant, it was in order of 1.34, 1.6 and 1.78 for pure POE oil, pure mineral oil and mineral oil + Al_2O_3 respectively.

Kumar et al. [15] conducted an experimental investigation on domestic refrigerator of refrigerating capacity 125L based on refrigerant R134a. The experimental setup was consist of hermetically sealed compressor, fan cooled condenser, expansion device (capillary tube) and an evaporator section (loaded with water). Service ports were provided at the inlet of expansion device and compressor for charging the refrigerant. The ambient temperature was ±1.5°C and air flow velocity was less than 0.35m/s. Al_2O_3 nanoparticles of 40-50 nm in diameter were dispersed

in PAG oil (compressor lubricant) and solution stability was achieved by magnetic stirrer and ultrasonic homogenizer. Nanolubricant with 0.2% concentration was fed to the experimental setup and the tests were conducted under the same conditions. Performance tests were also conducted with charged masses of 150gm., 180 gm. and 200gm. Mixing of Al_2O_3 nanoparticles in R134a showed enhancement in the COP of the refrigerator. Use for Nanolubricant reduced capillary tube length and found cost effective. With capillary length of 10.5 m, the maximum COP of around 3.5 was achieved. Moreover system consumed 10.32% less energy than pure lubricant and R134a combination. So the results showed improvement in heat transfer characteristics with the use of lubricant based nanofluid with Al_2O_3 nanoparticles. Thus use of Al_2O_3 nanoparticles in refrigerator compressor lubricating oil was found feasible.

Hafez et al. [16] carried out an investigation using CuO nanoparticles in R134a in the vapour compression system. The evaporating coefficient of heat transfer was experimentally evaluated. Test rig consist hermetically sealed compressor of 1 HP, water cooled condenser, expansion device and evaporator (dipped in water). At the condenser inlet a specific amount of oil having the particular amount of CuO nanoparticles were added to refrigerant line. This mixture of refrigerant and nanoparticles (nanorefrigerant) flows through the condenser, expansion device and in evaporator it evaporates with the help of hot water around the evaporator. During the experiment heat flux to evaporator was varied from 10 to 40 kW/m^2. The investigations were carried out using CuO nanoparticles concentrations in order of 0, 0.1, 0.2, 0.3, 0.4, 0.5, 0.55, 0.6, 0.8 and 1%. Nanoparticles of 15 to 70 nm were used for this study. It was found that the evaporating heat transfer coefficient increases linearly with increase in heat flux (applied to the evaporator) on the logarithmic scale up to 0.55% CuO nanoparticles concentration and then it found to be decreasing for all heat flux values. Further it was observed that the heat transfer

coefficient increases with size of nanoparticles upto 25 nm and beyond which it found to be decreasing with increase in particles size. This trend was followed for all heat flux values.

Bi et al. [17] conducted an experimental investigation on a domestic refrigerator of 228 L with hermetically sealed reciprocating compressor. The ambient temperature was kept constant with $\pm 0.5^{o}C$ minor fluctuations and the air velocity was less than 0.25 m/s. To prepare nanorefrigerant R600a was used as base fluid with TiO_2 nanoparticles and 60g of nanorefrigerant was charged into the system. The tests were carried out to evaluate energy consumption of refrigerator operates continuously for 24 hours with less than $5^{o}C$ average temperature of the food storage compartment and temperature of freezing compartment was less than $-18^{o}C$. Energy consumption was found to be 0.9567 kWh, 0.8999 kWh and 0.8649 kWh for R600a, R600a+TiO_2 (0.1 g/L) and R600a+TiO_2 (0.5 g/L) respectively. So with 0.1 g/L TiO_2 nanoparticles in base refrigerant the energy saving was 5.94% and with 0.5 g/L nanoparticles energy savings were found to be 9.6% as compared to pure R600a. Further discharge pressure of compressor was found lowest for R600a+ TiO_2 (0.5 g/L). After 40 mins the discharge pressure was found to be 5.7 bar for pure R600a whereas for 0.5 g/L nanorefrigerant the discharge pressure was around 5.4 bar. Similarly pressure at suction of compressor was also lowest in the case of 0.5 g/L nanorefrigerant. It was found 0.57 bar and 0.48 bar for pure R600a and 0.5 g/L nanorefrigerant respectively. The results also showed that the evaporation temperature was reduced in the case nanorefrigerant, which result lower frozen storage and food compartment temperatures. After 50 mins, for pure R600a the lower food compartment temperature was found to be $3.75^{o}C$, whereas it was $3.4^{o}C$ for 0.5 g/L nanorefrigerant. Frozen food storage compartment temperatures were in order of $-18.25^{o}C$, $-19.2^{o}C$ and $-19.5^{o}C$ for R600a+TiO_2 (0.1 g/L) and R600a+TiO_2 (0.5 g/L) respectively.

Loaiza et al. [18] conducted a numerical study studied in which use of nanofluids as secondary coolants in vapor compression refrigeration systems was studied. In inner circular section evaporator water based nanofluid (as secondary fluid) was supposed to flow and the flow of refrigerant was through the annular passage. The heat load was transferred to the secondary fluid and it rejects that heat to the refrigerant flowing through the evaporator. Modeling of heat exchanges was done by multi-zone method. For simulation the input data include the geometry of compressor and heat exchangers, nanofluid characteristics (base fluid, nanoparticle material, size and volume fraction), type of refrigerant, , inlet temperature of condenser coolant, inlet and outlet temperatures of secondary fluid (nanofluid), evaporating temperature, condensing temperature, degree of superheat at compressor inlet, degree of subcooling at condenser outlet and refrigeration heat load. The simulation was carried out for small capacity system working with four different water based nanofluids that include Al_2O_3, CuO, Cu and TiO_2. The volume fraction of nanoparticles in base fluid ranged from 1 % to 5% and particle size was varied from 10 to 50 nm. In this simulation study it was found that the greatest reduction in evaporator area can be obtained if Cu+H_2O nanofluid with lower particle diameters and large volume fractions used. Whereas water based nanofluid having CuO nanoparticles (as secondary refrigerant) requires more evaporating area followed by TiO_2 and Al_2O_3. Also power requirement was found to be less and considerable increase in COP. Moreover, the pressure drop in secondary loop was found to be increased with increase in volume fraction and particle size, which was due to increased viscosity. Pressure drop was observed highest for Cu and lowest for Al_2O_3.

Sabareesh et al. [19] carried out an experimental study on refrigerant R12 based vapour compression system. In this system mineral oil based nanofluid (nanolubricant) with small concentrations of TiO_2 (30-40 nm) was used as lubricant. This study found that addition of

nanoparticles to mineral oil (lubricant) increases the viscosity, but coefficient of friction was found to be decreasing with increase in volume concentration of nanoparticles. Volume fraction 0.01% was found optimum as it improved the rate of heat transfer by 3.6%. In addition to this the reduction in compressor work was observed, which was around 11%, hence this result increase in coefficient of performance (COP) by 17%. This study concluded that use of nanoparticles in lubricant is useful to improve the performance of vapour compression system.

Kumar et al. [20] conducted an experimental study in which vapour compression system was used with R600a as refrigerant. Three type of compressor lubricants were used in this investigation named as POE oil, mineral oil and nanolubricant (mineral oil + Al_2O_3). The mass fraction of Al_2O_3 nanoparticles was taken as 0.06% and average size was <50 nm. Evaporator pressure kept constant at 0.58 bar and condenser pressure was maintained at 5.6 bar. It was found that refrigerant R600a works normally with mineral oil based nanolubricant. Freezing capacity of refrigeration system was found to be improved with nanolubricant as compared to POE oil, whereas power consumption of compressor also found reduced by 11.5%. Ultimately coefficient of performance (COP) of system increased by 19.6%, when POE oil replaced with nanolubricant (mineral oil + Al_2O_3).

Clancy et al. [21] proposed a new design, where the heat transfer of a vapor compression system increased by increasing the thermal heat transfer properties of the refrigerant by using nanoparticles. Nanoparticles are mixed with refrigerant at inlet of the condenser and removed at outlet of condenser. A membrane or filter is fitted at the condenser outlet that collects the nanoparticles and these particles were re-circulated by means of recalculating pump to the condenser inlet. In this system any fluorocarbons, ammonia, water and sulfur dioxide can be

used as refrigerant. Al_2O_3, TiO_2, Fe_3O_4, CuO, carbon nanotubes (single or multi-wall) and gold can be used as nanoparticles either alone or in combination of several nanoparticles. The nanoparticles are suspended in the refrigerant along with surfactant to have a stable nanofluid. The diameter of particles is in the range of 1 nm to 100 nm. The recommended nanoparticles percentage should be less than 10% of fluid weight.

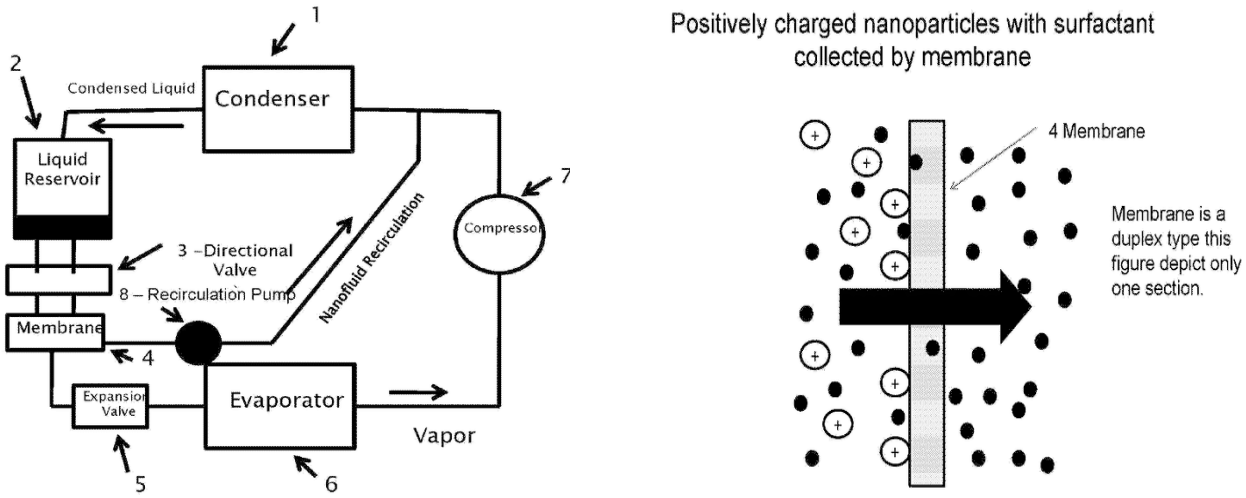

Flow diagram of the system Membrane working

Figure 2.1 – Design of developed model [21]

Mahbubul et al. [22] carried out a study to evaluate pressure drop characteristics of R123 based nanorefrigerant with TiO_2 nanoparticles (without surfactant) flowing through a horizontal smooth tube. The considered experimental conditions include 0-5 % volume concentration of nanoparticles, mass fluxes varied from 100 to 200 kg/m^{2}s and quality of vapour taken to be from 0.2 to 0.7 at 25^{o}C ambient temperature. It was found that the frictional pressure drop increases with increase in mass fractions of nanoparticles. Further, frictional pressure drop increases with increase in vapour quality. The pressure drop using R123+ TiO_2 (0.5 wt%) was found to be 1.30 kPa and 4.25 kPa for 0.2 and 0.7 vapour quality respectively at 100 kg/m^{2}s mass flux, whereas at

same conditions frictional pressure drop for pure R123 was found to be around 1.1 kPa. Same trend was found for all the three mass fluxes. It was also pointed out that, frictional pressure drop increased notably with mass fraction at lower mass fluxes than higher mass fluxes. Moreover the frictional pressure drop characteristics for different volume concentrations % of nanoparticles in base refrigerant R123 were also analyzed by varying concentration from 1-5 vol%. In this investigation it was found that pressure drop increases more rapidly with the increase in volume concentrations as compared to vapour quality. With 0.7 vapour quality and 100 kg/m^{2}s mass flux, the pressure drop was found to be 6 kPa/m, 9kPa/m and 300 kPa/m for R123, 1% v TiO_2, 5% v TiO_2 respectively, whereas at 0.6 vapour quality the pressure drop was found in order of 5 kPa, 8kPa and 100 kPa for R123, 1% v TiO_2, 5% v TiO_2 respectively.

Peng et al. [23] carried out a study to evaluate frictional pressure drop for nanorefrigerant during flow boiling through a horizontal smooth tube. In this study refrigerant R113a was used as base fluid in which CuO nanoparticles of 40nm size were suspended. Mass fractions of nanoparticles were taken as 0.1%, 0.2%, and 0.5%. During this experiment it was found that is the friction pressure drop for R113 + CuO mixture is larger than that of pure R113 refrigerant and with increase in the mass fraction of nanoparticles in refrigerant the pressure drop also increases. The maximum increase of frictional pressure drop was found to be around 20.8% for 0.5% nanoparticles concentration.

Kedzierski et al. [24] carried out an investigation to measure liquid kinematic viscosity and density of synthetic polyolester (chiller lubricant) based nanolubricant having Aluminium oxide (Al_2O_3) nanoparticles over the temperature ranged from 288 K to 318 K at atmospheric pressure. Al_2O_3 nanoparticles with diameters 10 nm and 60 nm were used in this study along with

surfactant. This study setup a new model to estimate the kinematic viscosity of the nanolubricant by summing up the viscosities of base lubricant, nanoparticles and surfactant. The effect of particle mass fraction, temperature, mass fraction of surfactant and particle size on kinematic viscosity of nanolubricant was studied. The liquid density of nanorefrigerant was found to be decreased with increase in temperature. Moreover, liquid density was also seen to be increasing with increase in mass fraction of Al_2O_3 in base lubricant. Further, kinematic viscosity was found to be decreasing with increase in temperature for both sizes (10 nm and 60 nm) and all mass fractions of Al_2O_3 nanoparticles.

Parise et al. [25] developed the simulation model to predict the performance of vapour compression heat pump in which nanofluids were used as condenser coolants. Test rig was assembled for this purpose that consist a heat pump (liquid-to-liquid) of 19 kW capacity, hermetically sealed reciprocating compressor, double-tube condenser and evaporator (counter flow type) and a thermostatic expansion valve. The condenser of system was divided into three zones termed as de-superheating, condensing and sub cooling, whereas the evaporator was divided into boiling and superheating zones. Inlet states and mass flow rates were also added in the equations of this model. These equations were solved with the help of computational model and overall thermal performance for cycle, as well as thermodynamic states of refrigerant and condensing/evaporating pressures were evaluated. Simulation was done for water-to-water heat pump and then water was replaced by water based nanofluid having Cu nanoparticles. In this investigation it was found that with 2% volume fraction of Cu nanoparticles in water, the heat transfer coefficient can be improved by 5.4%.

Peng et. al. [26] reported an investigation, which has also been done on the heat transfer characteristics of refrigerant + nanolubricant mixture with diamond nano particles during nucleate pool boiling. R113 was used as refrigerant and VG68 was used as oil. In this study the heat transfer coefficient of R113 + oil + diamond nanoparticles was found to be greater than the R113 + oil mixture during nucleate pool boiling. This study also proposed a correlation to find out the heat transfer coefficient during nucleate pool boiling of refrigerant + nanolubricant. This correlation satisfied their experimental results well.

Table 2.1 – Summary of literature review

Year	**Investigator**	**Refrigerant and Nanoparticles**	**Size (nm)**	**% volume concentr-ation or mass fraction**	**Performance**
2007	Bi et al. [12]	R134a + TiO_2	–	0.1%	Reduction in energy consumption by 26.1%.
2007	Park et al. [6]	R123, R134a + CNT	20	1.00%	Heat transfer coefficient enhancement up to 36.6%.
2009	Jwo et al. [13]	R134a + Al_2O_3	–	0.1%	2.4% reduction in energy consumption and 4.4% improvement in COP
2009	Trisaksri et al. [7]	R141b + TiO_2	21	0.01%, 0.03%, 0.05%	Nucleate pool boiling heat transfer deteriorated with increasing particle concentrations.
2009	Hao et al. [8]	R113 + CuO	40	0.15–1.5%	Maximum enhancement of heat transfer coefficient, 29.7%.
2009	Peng et al. [23]	R113 + CuO	40	0.1%, 0.2%, 0.5%	Frictional pressure drop increased by 20.8%.

2009	Kedzierski et al. [11]	R134a + CuO	30	0.50%	Enhancement of heat transfer coefficient of between 50% and 275%. Improvement decreases with increase in nanolubricant concentration.
2010	Hao et al. [9]	R113 + Diamond	10	0-5%	Nucleate pool boiling heat transfer coefficient increased by 63.4%.
2010	Peng et al. [26]	R113 + Diamond	20-50	–	Improvement in nucleate pool boiling heat transfer characteristics.
2010	Loaiza et al. [16]	H2O + Cu, Al_2O_3, CuO, TiO_2	10-50	1-5%	Reduction in evaporator area - Cu ($0.238m^2$), followed by CuO ($0.250m^2$), TiO_2 ($0.251m^2$) and Al_2O_3 ($0.256m^2$) results increase in COP.
2011	Subramani et al. [14]	R134a + Al_2O_3	50	0.06%	28% time reduction to bring down temperature, 28% reduction in power consumption and 33% increase in COP by Nanolubricant.
2011	Bi et al. [17]	R600a + TiO_2	50	0.1-0.5 g/L	Reduction in power consumption by 5.94% to 9.6%, lower evaporating temperatures were achieved with reduced compressor pressures
2012	Kumar et al. [15]	R134a + Al_2O_3	50	0.20%	10.32% reduction in power consumption and 12% increase in COP by Nanolubricant.
2011	Hafez et al. [18]	R134a + CuO	15-70	0.1-1%	Heat transfer coefficient increases linearly with heat flux upto 0.55% CuO and increases with CuO nanoparticle size up to 25nm and then decreases with size.

2011	Mahbubul et al. [22]	R123 + TiO_2	–	0.05-1%	Pressure gradient increases rapidly with the increment of volume concentrations compared to vapor quality
2012	Parise et al. [25]	H_2O + Cu	–	2%	Improvement in heat transfer coefficient by 5.4%.
2012	Clancy et. al. [21]	Freon+Al_2O_3, TiO_2, Fe_3O_4, CuO, CNT	1-100	0-10%	Proposed new design which uses nanoparticles in condenser only results improvement in condenser heat transfer properties.
2013	Kumar et al. [20]	R600a + Al_2O_3	50	0.06%	Improvement in freezing capacity, energy reduction by 11.5% and COP improved by 19.6%.
2012	Sabareesh et al. [19]	R12 + TiO_2	30-40	0.005-0.015%	Optimum value of volume fraction was found as 0.01% which lead to increase in heat transfer by 3.6%, reduction in power consumption by 11% and improvement in COP by 17%.
2013	Kedzierski et al. [24]	Lubricant + Al_2O_3	10 & 60	0.05-0.35%	Density of nanolubricant increases with increase in mass fraction and kinematic viscosity decreases with mass fraction
2014	Coumaressin et al. [10]	R134a + CuO	10-70	0.05-1%	Evaporating heat transfer coefficient improved upto 0.55% concentration

2.2 GAP STUDY AND OBJECTIVES

2.2.1 Gap Study

Based on literature review the following key issues have been highlighted which are needed to be addressed:-

(i) Direct mixing of nanoparticles with Refrigerant R134a has not been done in vapour compression cycle

(ii) Not much work has been reported on R134a-Al_2O_3 combination over varying conditions

(iii) An improvement with nanoparticle mass fractions at different concentrations is not clearly understood which needed a detailed investigation

(iv) An effect of ambient temperature on the performance of nanorefrigerant based vapour compression system has not been studied

(v) Effect of variation in evaporator heat load and refrigerant mass flow rate on system performance is available in very few literatures

(vi) A limited work has been reported on small capacity domestic refrigerators

(vii) A very limited literature with experimental data for nanorefrigerant based system

2.2.2 Study Objectives

Based upon the gap study following objectives have been decided. An attempt has been made in order to understand and investigate the issues related to the performance of the refrigeration system.

(i) To evaluate the performance of a vapour compression system using a nanorefrigerant prepared by direct dispersion of Al_2O_3 nanoparticles into the base refrigerant 134a

(ii) To study the effect of ambient temperature on the performance of vapour compression system using both pure refrigerant R134a and nanorefrigerant (R134a+Al_2O_3)

(iii) To study the effect of different mass concentrations of nanoparticles (Al_2O_3) on the performance of the refrigeration system

(iv) To study the performance of the refrigeration system under varying evaporator heat load

(v) To study the performance of the refrigeration system under varying volume flow rates of the refrigerant/nanorefrigerant (R134a+Al_2O_3)

CHAPTER - 3

EXPERIMENTAL SETUP AND TEST PROCEDURE

Literature review shows that the application of nanofluid in refrigeration system is quite feasible and an effective way to enhance its heat transfer performance. So, based on literature review R134a based nanofluid with Al_2O_3 nanoparticles has been selected for proposed study. A test rig as per Indian standard has been designed and assembled to conduct the experimental investigations.

3.1 EXPERIMENTAL SETUP

An experimental setup of vapour compression refrigeration system has been fabricated to carry out the experiments. System is very much similar to domestic refrigerator (165 ltr). The detail about its different parts is as follows.

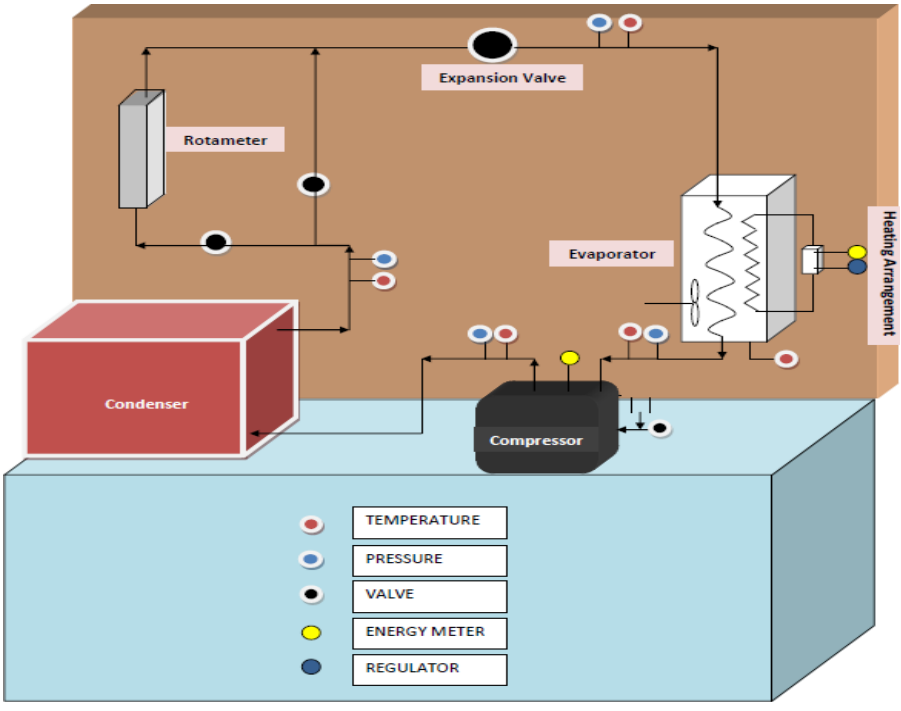

Figure 3.1 - 3D model of experimental setup

3.1.1 – System Layout

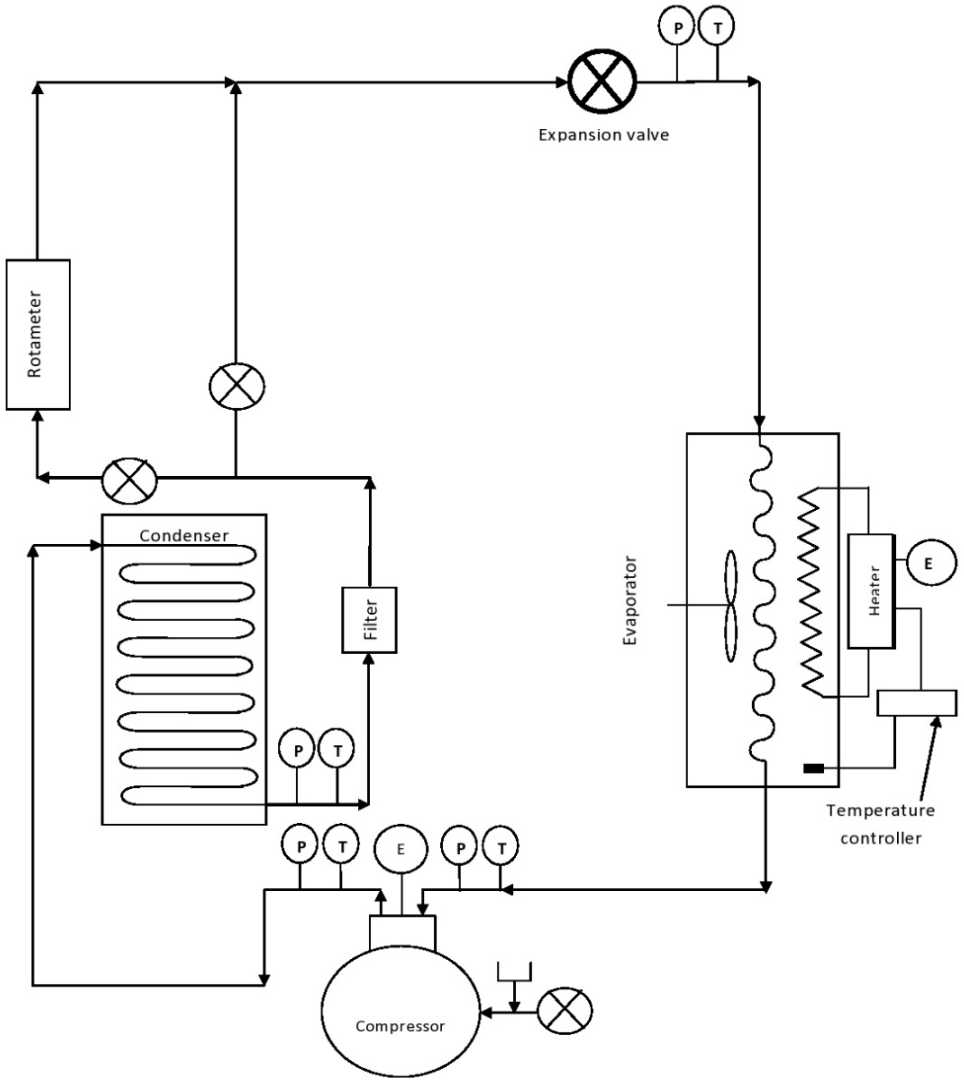

Figure 3.2 – System layout of experimental setup

Figure 3.2 show the layout and schematic arrangement of experimental test rig, the hermetically sealed compressor is provided with the charging line through with the refrigerant is charged into the system. The low pressure and low temperature refrigerant vapours (saturated or superheated) coming out of evaporator are compressed in compressor to high pressure and high temperature vapours. Then these vapours enter into the air cooled condenser (with natural convection) where

it rejects its latent heat of vaporization at constant pressure and changes to high pressure liquid refrigerant. Then after passing through filter it enters to the rotameter, which is installed to measure volume flow rate of refrigerant (litre per hour - LPH). The rotameter is installed in parallel, so that it can be repaired by diverting the flow. After passing through rotameter the high pressure liquid refrigerant enters into the hand operated expansion value where the free expansion of liquid refrigerant takes place. After expansion the high pressure and high temperature liquid refrigerant converted into low pressure and low temperature liquid + vapour mixture (major part liquid). Expansion valve is followed by evaporator. The evaporator coil is submerged in water container having 10.5 litres of water. A 230 W heater is also fitted in container to give desired heat flux to water. In order to maintain desired temperature of water the heater is operated by a temperature sensor, which senses the water temperature and accordingly controls the power supply to the heater through relay. The system is fitted with four pressure gauges and thermometers in order to measure the pressure and temperature of all salient points, e.g. at suction and discharge of compressor, outlet of condenser and after expansion.

S. No.	Component	Qty.
1	Compressor	1
2	Condenser	1
3	Evaporator	1
4	Expansion Device (Manual)	1
5	Filter	1
6	Heating Element	1
7	Temperature Gauge (Thermometer)	5
8	Pressure Gauge	4

9	Rotameter	1
10	Energy Meter	2
11	Ampere Meter	1
12	Voltmeter	1
13	Digital Temperature Controller	1
14	Hand shut value	4

Table 3.1 – List of components

Figure 3.3 – Actual picture of experimental setup

3.1.2 Details of Components

(i) Compressor – Compressor is installed after evaporator and before condenser. The basic function of compressor is to raise temperature and pressure of refrigerant vapours coming out of evaporator. The vapours leaving the compressor have superheated state with high pressure and high temperature, this enable refrigerant to reject heat to environment. Compressor is also responsible for circulation of refrigerant in system. For this experimental setup the hermetically sealed reciprocating compressor has been used with R134a refrigerant. This model is commercially used in 165 litre capacity domestic refrigerators.

Description	**Specifications**	
Manufacturer	Godrej & Boyce Mfg. Co. Ltd.	
Model	POWER COOL COMP R134a G1-1+CAPCT	
Dimensions	m*m*m	0.201*0.164*0.175
Capacity	Btu/hr.	410
Motor input	Watts	107
EER	Btu/W hr.	3.83
Displacement	Cc	4.6
Voltage range	V	150-260
L.V. Pickup	V	160V
Oil Charge	Cc	300
Net Weight	Kg	7.8
Overload protector		OLPA

Table 3.2 – Compressor specifications

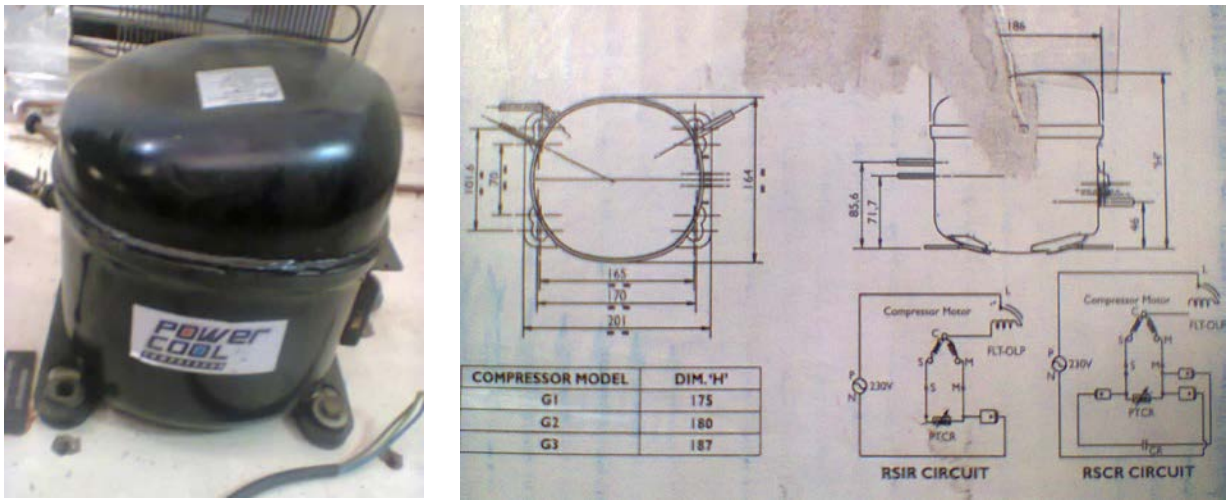

Figure 3.4 – Actual compressor picture and circuit diagram

(ii) Condenser - Condenser a device or unit used to condense vapour refrigerant into liquid refrigerant. This is installed after compressor, the high temperature and high pressure vapour refrigerant from compressor passes through the condenser, where it rejects latent heat of vaporization. The heat removed in condenser is sum of heat extracted from evaporator space and heat added in compressor. Subcooling can be achieved in condenser by removing heat below the saturation liquid temperature (sensible cooling). In this experimental setup the wire and tube type naturally air cooled condenser is used, whose specifications are as under.

Description	**Specification**
Type	Air cooled - Wire tube type (Natural Convection)
Diameter of Pipe	0.00635 m
Length of Pipe	13.7 m
Area of Condenser	0.2732 m^2
Material	Copper

Table 3.3 – Condenser specifications

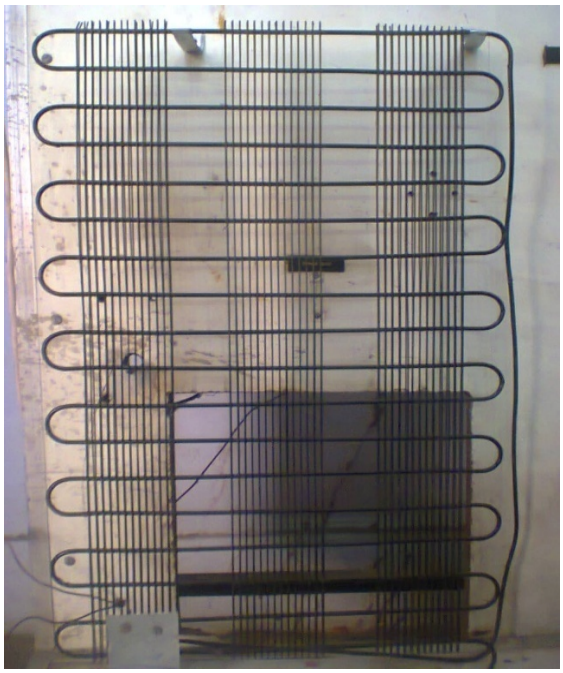

Figure 3.5 - Wire tube condenser

(iii) Filter - Any impurity present in refrigerant or entered at the time of charging may cause the blockage of refrigerant flow. So to obstruct any impurity present in the system filter is used. Filter is located between condenser and expansion valve. In this section the refrigerant is in liquid phase so it is easy to filter it.

Figure 3.6 - Filter

(iv) Expansion valve - The expansion valve is located between condenser and evaporator. It has two jobs to perform. It allows liquid refrigerant to enter the evaporator and at the same time maintains the required pressure in the evaporator. The high pressure liquid refrigerant coming out of condenser enters the expansion valve where the isenthalpic expansion takes place, so no work is obtained from the expansion process. The refrigerant leaving the expansion valve is in liquid form mainly, but little amount of refrigerant also converted to vapour. The state of liquid vapour mixture is nearly saturated. Most of the commercial refrigeration systems use capillary tube as expansion valve as it is cheaper and operation is simple. But in this experimental study the variation of flow rate is required so hand operated expansion valve is used in this setup in order to vary volume flow rate of refrigerant passing through the evaporator.

Figure 3.7 - Hand operated expansion valve

(v) Evaporator - The liquid refrigerant entering the evaporator from the refrigerant flow control is suddenly under low pressure. This makes it vaporize and absorb heat and produce refrigeration effect.

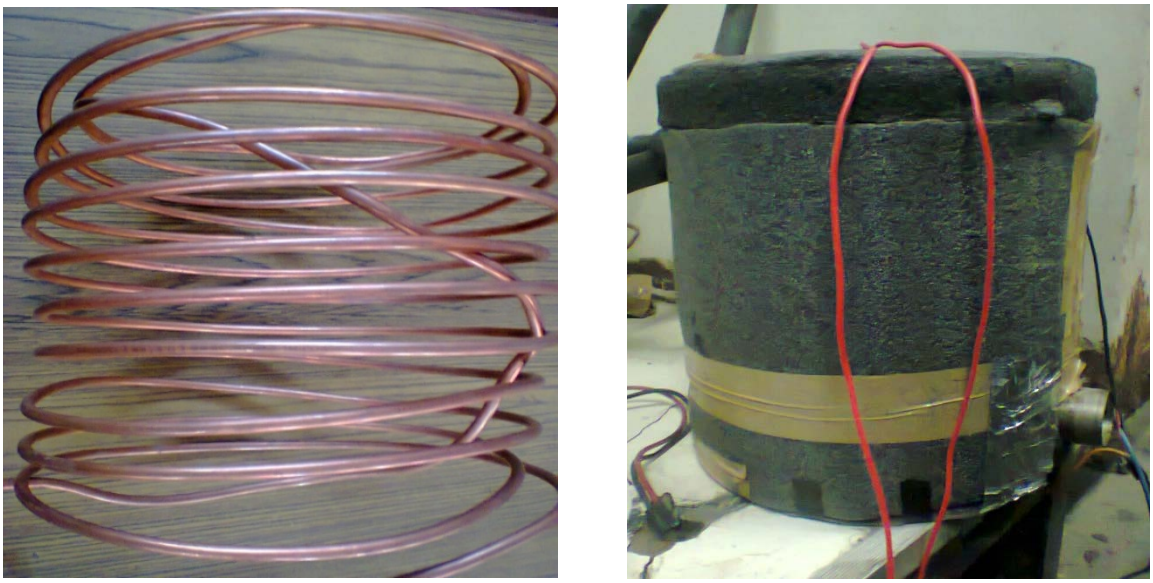

Figure 3.8 – Evaporator coil and evaporator container with water

First the copper pipe has been taken and a coil is formed from it as shown in Figure 3.7. This coil is then placed into container (for water) and connections are made with expansion valve outlet and compressor inlet with the help of brazing.

Description	**Specification**
Type	Emersion coil type
Dia. of Pipe	0.00635m
Length of Pipe	7.62m
Area of Evaporator	$0.152m^2$
Material	Copper

Table 3.4 – Evaporator specifications

(vi) Heating element - As it is required to vary the heat flux to the evaporator, a heating element is used to heat the water in which the evaporator coil is immersed. A temperature control system is installed to control the temperature in container which operates the heater. By this way measured

heat is absorbed by evaporator and hence with this refrigerating effect can be calculated. Heater gets ON/OFF as per requirement to maintain desired temperature in container.

Description	**Specification**
Specification	230V,50Hz A/C
Power	230W

Table 3.5 – Heater specifications

Figure 3.9 – Heating element

(vii) Pressure gauge - To measure the pressure of the R-134a Refrigerant at different points as shown in layout. The bourdon gauge pressure gauges are used in this experimental setup. There are two regions in vapour compression system known as:

High pressure side – between compressor outlet and expansion valve inlet

Low pressure side - between expansion valve outlet and compressor inlet

Pressure Gauge	Range	Qty.
High Pressure Side	0-300 psi	2
Low Pressure Side	(-30) - 150 psi	2

Table 3.6 – Pressure gauges specifications

Figure 3.10 – Pressure gauge

(viii) Refrigerant - In the experimental setup it has been decided to use R-134a refrigerant, due to reason of its wide commercial use and acceptability. R134a is commonly used refrigerant in domestic refrigerators and cars. Specifications of used refrigerant are listed below.

Description	Specification
Manufacturer	Seattle Gas, Italy
Purity	0.999
Moisture	5ppm(max)
Acidity	0.1ppm(max)
Vapour residue	100ppm (max)
Product	1.1.1.2-Tetraflouroethane

Table 3.7 – Refrigerant specifications

Figure 3.11 – Refrigerant R-134a cylinder

(ix) Rotameter - A Rotameter is a device that measures the flow rate of liquid or gas in a closed tube. It belongs to a class of meters called variable area meters, which measure flow rate by allowing the cross-sectional area the fluid travels through to vary, causing some measurable effect. In this setup we have used glass tube rotameter which is located between condenser and expansion valve. The rotameter is installed in parallel (refer layout), so that flow through it can be diverted in case of repairing.

Description	**Specification**
Manufacturer	ZEST ENGINEERING
Type	Glass tube rotameter
Range	0-40 LPH

Table 3.8 – Rotameter specifications

Figure 3.12 – Glass tube rotameter

(x) Voltmeter - To measure supply voltage needle type voltmeter is used.

Description	**Specification**
Manufacturer	ESS VEE Electricals
Type	72 sq mm
Range	0-300 V

Table 3.9 – Voltmeter specifications

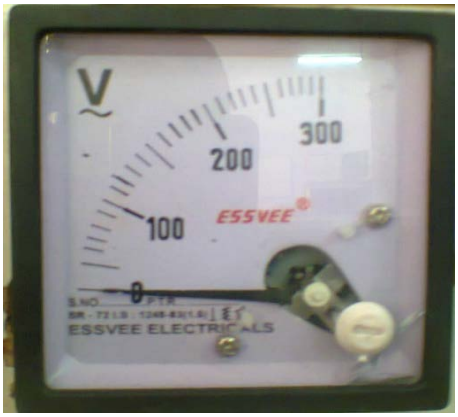

Figure 3.13 – Voltmeter

(xi) Ampere meter - It has been used to measure the current requirement if the system. For this purpose digital ampere meter has been used.

Description	**Specification**
Manufacturer	Pyrotron
Type	Digital
Range	0-15 amp

Table 3.10 – Ampere meter specifications

Figure 3.14 – Ampere meter

(xii) Energy meter - It has been used to measure power input to the system. There are two energy meters used in the system, one is to measure energy consumption of compressor and other for heater.

Description	**Specification**
Manufacturer	Jaipur Metals and Electricals
Type	AC, 1 Phase, 2 wire, 50Hz

Range	0-20 amp
Rev/kWh	600

Table 3.11 - Energy meter specifications

Figure 3.15 – Energy meter

(xiii) Digital temperature controller - In water drum (in which evaporator immersed), it is required to maintain a particular temperature, so for this purpose digital temperature controller is used to cut off the heater supply when desired temperature achieved. This controller guides the relay which results heater ON/OFF.

Figure 3.16 – Digital temperature controller and relay switch

Description	Specification
Manufacturer	ACR Inst & Valve Pvt. Ltd.
Type	Digital
Range	-40^{o}C – 50^{o}C

Table 3.12 – Temperature controller specifications

(xiv) Hand shut valve - These are hand operated valves which are used to close the flow in the line. Four valves of this type are used, at charging line and both ends of rotameter. As rotameter is installed in parallel, so if the flow is to be bypassed then these values can be used to divert the flow (refer Figure 3.17).

Figure 3.17 - Hand shut valve

(xv) Temperature gauges (mercury thermometers) - To measure the temperatures at all salient points mercury thermometers are used. These are installed at compressor outlet, condenser outlet, after expansion valve, evaporator outlet.

3.1.3 Other Materials, Connections and Tool Used

Tubing

The refrigeration and air conditioning systems mostly use copper tubing. Soft copper tubing is used in some commercial refrigeration and air conditioning work, whereas steel tubing is used with Ammonia. Copper is a soft and ductile material, so it is easy to bend and make flare on copper tubing. Moreover copper have notable resistance to corrosion and it do not react with refrigerant. These tubes are generally available in rolls of 25, 50 and 100 feet long [31]. For this experimental test rig, ¼" copper tubing has been used.

Figure 3.18 - Copper tubing [31]

Tubing Connections

(i) Flared Connections

(ii) Soldered or Brazed Connections

(i) Flared Connections - Flare connections are a kind of compression fitting which are generally used to connect metal tubing in refrigeration systems. This type of joint requires softer and ductile material hence it is commonly used for soft steel and copper. Tube flaring can be considered as a type of forging operation with usually includes cold working procedures. After producing flares a flare nut is used to join the flared tubing to fitting. The flared joints are leak proof and pressure resistant with high degree of long term reliability. The tool used to flare tubing includes a die to grip the tube and a mandrel which is forced into the tube end to produce flare. The 45-degree SAE style is most commonly used flare fitting standards, whereas the AN/JIC style is commonly used in higher pressure applications for given tubing size. Moreover AN/JIC and SAE fittings are completely incompatible due to difference in flare angles. Further, JIC and AN fittings are not interchangeable for design controlled applications due to different quality standards [32].

Figure 3.19 - Flared connections [32]

Figure 3.20 - Flared type fittings [31]

(ii) Brazed or Soldered Connections - Brazing is a metal joining process in which filler metal is heated above its melting point and applied between two fitting pipes with the help of capillary action. In brazing operation the filler metal is heated slightly above its melting point and flux is use to protect it from atmosphere. After this filler metal flows over the base metal and parts are joined together after cooling. Soldering is similar to brazing except the temperatures used to melt the filler metal are lower in case of soldering. Joints obtained by soldering are used for drains and water pipes. Sometimes silver brazed joints are used for refrigeration tubing [33].

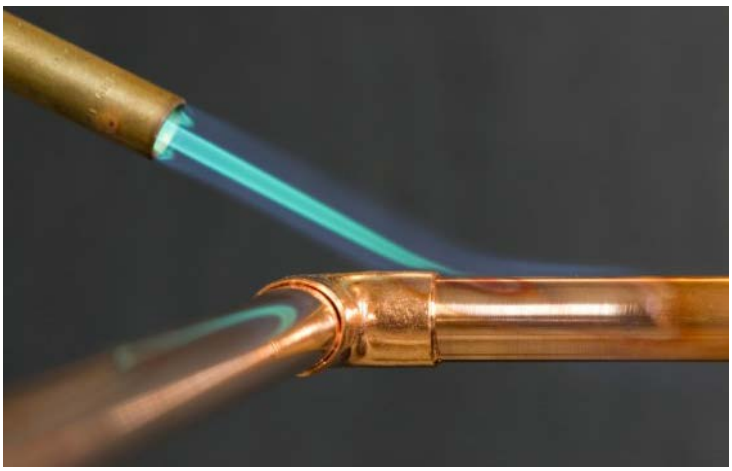

Figure 3.21 - Brazed tubing [31]

1	Wrenches	11	Hacksaws
2	Vises	12	Pliers
3	Abrasives	13	Screw drivers
4	Files	14	Taps
5	Hammers	15	Dies
6	Mallets	16	Cleaning solvents
7	Twist drills	17	Gaskets
8	Measuring rules and tapes	18	Service Valves
9	Brushes	19	Cold Chisels
10	Stamps	20	Fastening Devices

Table 3.13 – List of hand tools used

3.2 TEST PROCEDURE AND METHODOLOGY

To study the performance of nanorefrigerant (R134a + Al_2O_3) based vapour compression refrigeration system, following test procedure has been adopted.

Refrigerant – R134a

Nanoparticle material – Aluminium Oxide (Al_2O_3)

Nanoparticle size – 20nm

3.2.1 Parameters to be Varied – To study the effect on performance following parameters have been varied:-

(i) Mass fraction of nanoparticles - The mass fraction of nanoparticles dispersed in base refrigerant results a significant effect on heat transfer properties, hence on performance. So two mass fractions have been taken for this study as 0.5% and 1%/gm of refrigerant.

(ii) Heat flux - The performance of the system is greatly influenced by the state or quality of vapours entering the compressor. It directly affects the compressor work e.g. superheated vapours needs more compressor work. Thus to study this phenomenon the evaporator of the refrigeration system has been placed in water, so by heating water (by means of heater) the measured heat flux has been given to evaporator coil and the same will be varied by adjusting temperature of thermal load (water). Temperature taken is 15-17^oC and 30-31^oC.

(iii) Volume flow rate - The refrigerant volume flow rate through the evaporator also affect the refrigeration system performance. So the volume flow rate has been regulated by using hand operated expansion valve. The volume flow rate has been measured with help of the Rotameter. Flow rates taken (in Litre/hr) – 6.5 LPH and 11 LPH.

(iv) Ambient temperature - The variation in room temperature also affects the system performance. At colder or lower ambient temperatures system will work more efficiently

than system operating at higher ambient. This is due increase in operating temperature for compressor and the temperature gradient across the condenser has also been decreased (specifically in case of air cooled condensers). Hence to study the effect of ambient temperature on various performance parameters has also been investigated by operating system at 21 ^{o}C ±1^{o}C and 28 ^{o}C ±1^{o}C room temperatures.

3.2.2 Performance Parameters to be Studied – Following parameters to be examined to evaluate their effect on the performance of refrigeration system:-

(i) Coefficient of Performance (COP)

(ii) Cooling capacity - Time required to achieve a desired temperature

(iii) Power consumption

(iv) Temperature drop in condenser

(v) Temperature gain in evaporator

(vi) Temp. at all points, such as across condenser, evaporator, compressor inlet and outlet

3.2.3 Methodology – Following points explain the step by step procedure to work on the refrigeration system:-

(i) Firstly at 21 ^{o}C ±1^{o}C ambient temperature, vacuum has been created with the help of external compressor to withdraw air and moisture from the refrigeration system

(ii) After system evacuation pure refrigerant 100 gm of R134a has been charged into the system and measurement of above performance parameters are measured by varying the different parameters (mentioned above)

(iii) After collecting data for pure R134a, the refrigerant is discharged from the system and again system evacuation is done

(iv) Now measured mass fraction of 0.5gm (0.5%) of Al_2O_3 nanoparticles along with 100 gm of refrigerant has been charged into the system. Now the same procedure is repeated to collect the data with nanorefrigerant (R134a + Al_2O_3)

(v) The mass fraction of Al_2O_3 nanoparticles in nanorefrigerant has been further increased to 1gm (1%) and same procedure has been followed again

(vi) The above procedure has been repeated at increased ambient temperature around 28 ^oC $\pm 1^oC$

(vii) Now summarizing all different reading, desired performance parameters have calculated for different heat fluxes, mass fractions, refrigerant volume flow rates and ambient temperatures. Then the results have been compared by plotting different graphs

(viii) Furthermore after analyzing the performance, the conclusions of the experimental study have been derived

3.3 PROPERTIES OF BASE REFRIGERANT R134A

R134a (1,1,1,2-Tetrafluoroethaneis) is a haloalkane refrigerant which is having similar thermophysical properties to R12, but the potential of ozone layer depletion is less than R12. Its numerical designation is R134a or Isobutene and chemical formula is CH_2FCF_3. R134a is primarily used in domestic refrigerators and automobile air conditioning. It usually stored in light blue colored cylinders [27].

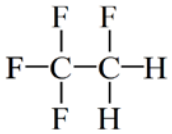

Figure 3.22 – Molecular structure of R134a [27]

Property	**Description**
Molecular weight	102.03 g/mol
Melting point (1.013 bar)	101 °C
Liquid phase	
Liquid density (1.013 bar and 25 °C (77 °F))	1206 kg/m3
Boiling point (1.013 bar)	-26.55 °C
Latent heat of vaporization (1.013 bar at boiling point)	215.9 kJ/kg
Vapor pressure (at 20 °C or 68 °F)	5.7 bar
Vapor pressure (at 5 °C or 41 °F)	3.5 bar
Vapor pressure (at 15 °C or 59 °F)	4.9 bar
Vapor pressure (at 50 °C or 122 °F)	13.2 bar
Critical point	
Critical temperature	100.95 °C
Critical pressure	40.6 bar
Critical density	512 kg/m3
Triple point temperature	103.3 °C
Gaseous phase	
Gas density (1.013 bar at boiling point)	5.28 kg/m3
Gas density (1.013 bar and 15 °C (59 °F))	4.25 kg/m3
Compressibility Factor (Z) (1.013 bar and 15 °C (59 °F))	1
Specific gravity	3.25
Specific volume (1.013 bar and 15 °C (59 °F))	0.235 m3/kg
Heat capacity at constant pressure (C_p) (1.013 bar and 25 °C (77 °F))	0.08754 kJ/(mol.K)

Miscellaneous	
Solubility in water (1.013 bar and 25 °C (77 °F))	0.21 vol/vol

Table 3.14 - Thermophysical properties of R134a [28]

3.4 PROPERTIES OF ALUMINA (Al_2O_3) NANOPARTICLES

Aluminium is considered as very good conductor of heat with excellent heat transfer properties. Nowadays Aluminum Oxide (Al_2O_3) nanopowder is widely used in research work that is going on heat transfer characteristics enhancement. In periodic table Aluminum is found in block P as period 3rd element, while oxygen is a block P, period 2 element. The morphology of aluminum oxide nanoparticles is spherical, and they appear as a white powder [3]. Its properties includes:-

Chemical Data	
Chemical symbol	Al_2O_3
Group	Aluminium 13
	Oxygen 16
Electronic configuration	Aluminium [Ne] $3s^2 3p^1$
	Oxygen [He] $2s^2\ 2p^4$

Table 3.15 - Chemical properties of Al_2O_3 [20]

Property	**Description**
Melting Point	2072°C
Boiling Point	2977°C
Colour	Ivory / White
Density	0.26 g/cm^3

Specific heat	880 J/KgK
Thermal conductivity	30 W/mK
Molecular mass	101.96 g/mol
Specific Surface Area	0.5- 50 m^2/g
Appearance	White powder
pH	7-9

Table 3.16 - Thermophysical properties of Al_2O_3 [20]

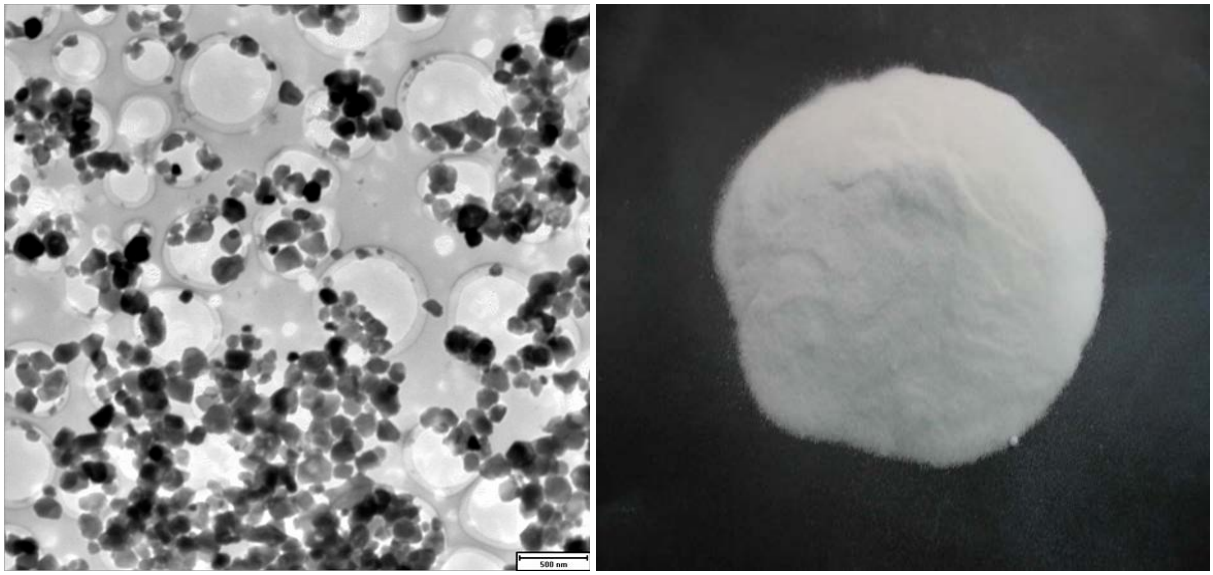

Figure 3.23 – Crystal structure and appearance of nanopowder [3]

In addition to these properties, it has also feature like insoluble in water, stable under normal pressure and temperature and it is odorless.

3.4.1 XRD and TEM of Al_2O_3 nanoparticles

X-ray diffraction (XRD) is a technique used to identify the atomic and molecular structure of a crystal. This method is also known as X-ray crystallography. In this technique incident X-rays beam has been diffracted into many directions by crystalline atoms. After determining the

intensities and angles of these beams a 3D picture of density of the crystal has been determined by crystallographer [29]. Transmission electron microscopy (TEM) is a technique to microcopy. In this method beam of electrons is transmitted through the specimen, it interact with specimen as it passes through. Then the image is generated from this interaction of electron. The high resolution image can be generated with help of TEM as compared to SEM or other techniques. The fine details can be achieved by this even as small as single column of atoms. Figure 3.24 shows the XRD and TEM results for used Al_2O_3 nanoparticles. As specified the resolution of TEM is 100nm [30].

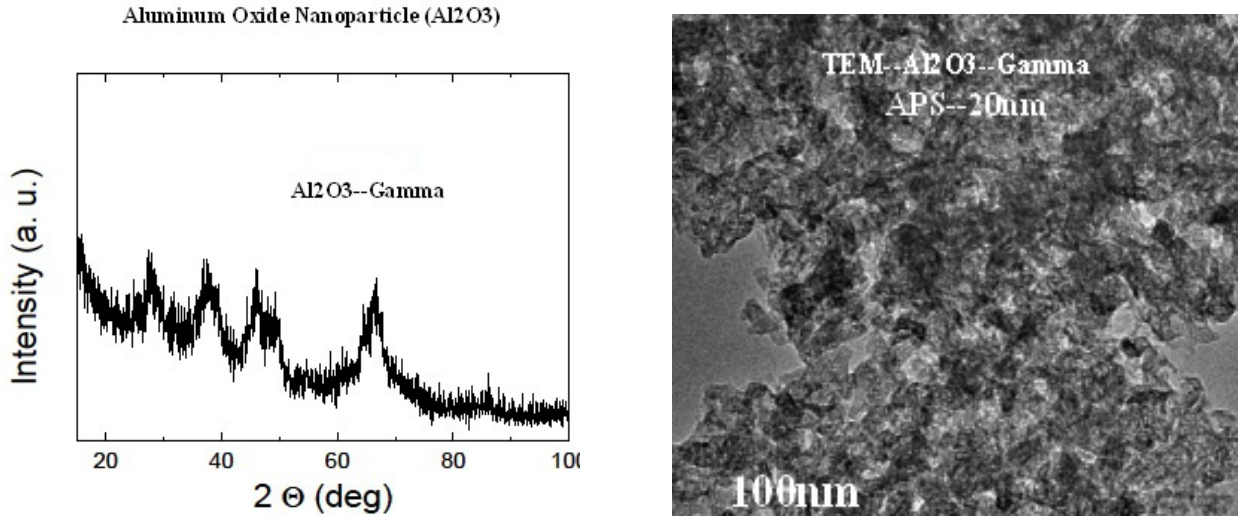

Figure 3.24 – XRD and TEM of Al_2O_3 (20nm) nanoparticles

CHAPTER - 4

RESULTS AND DISCUSSION

An experimental study has been carried out on nanorefrigerant (R134a + Al_2O_3) based refrigeration system. In this investigation R134a is taken as base fluid and Al_2O_3 (20nm) as a nanopowder. Various samples of nanofluids have been tested on experimental test setup. System performance has been studied by evaluating COP, time taken to achieve a desired temperature in evaporator, power consumption, refrigerant temperature drop in condenser and refrigerant temperature gain in evaporator. All these parameters are investigated at two different ambient temperatures (21 ^oC $\pm 1^oC$ and 28 ^oC $\pm 1^oC$), with two heat fluxes (at 15-17^oC and at 30-31^oC) and with two refrigerant mass flow rates (6.5 LPH and 11 LPH). Firstly the experiments are performed with base refrigerant R134a and then same investigation has been done with R134a + 0.5% Al_2O_3 and R134a + 1% Al_2O_3 samples.

4.1 COEFFICIENT OF PERFORMANCE (COP)

The term coefficient of performance (COP) is used to quantify the performance of refrigerator. Like power cycle efficiency, the COP is defined as the ratio of heat extracted in the refrigerator to work requirement of the system.

$$\text{COP} = \frac{\text{Refrigeration Effect (Q)}}{\text{Work Done (W)}}$$

COP is influenced by operating conditions, especially ambient temperature and relative temperatures between sink and source. Here in this experimental study actual COP of refrigeration system has been investigated.

Firstly the experiment is performed with 6.5 LPH volume flow rate of refrigerant maintaining constant evaporator load temperature around 15-17^{o}C and ambient temperature 21^{o}C ±1^{o}C. As Figure 4.1 shows, the COP with pure R134a is found to be 0.982 whereas with R134a + 0.5% Al_2O_3 and R134a + 1% Al_2O_3, COP is 1.065 and 0.929 respectively. So it is found that, by using R134a + 0.5% Al_2O_3 nanorefrigerant sample COP is improved by 8.49% and with R134a + 1% Al_2O_3 COP is decreased by 5.42% when compared to COP of pure refrigerant R134a.

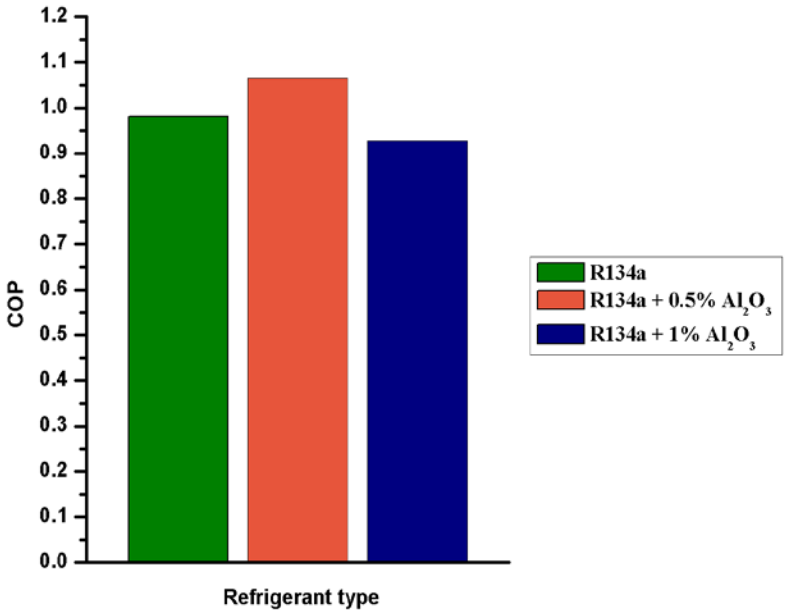

Figure 4.1 – COP comparison for system operating with 6.5 LPH volume flow rate, evaporator load at 15-17^{o}C and at 21^{o}C ±1^{o}C ambient temperature

As shown in Figure 4.2, at 28^{o}C ±1^{o}C ambient temperature, COP with pure R134a is found to be 0.855 and with nanorefrigerant having 0.5% Al_2O_3 and 1% Al_2O_3, COP is 0.935 and 0.780 respectively. So when pure R134a COP is compared with R134a + 0.5% Al_2O_3, then it has found COP has been improved by 9.39%. Whereas with R134a + 1% Al_2O_3, COP is found to be decreasing by 8.67% compared to pure refrigerant (R134a). Hence, it has been noticed that

higher mass fraction of Al_2O_3 nanoparticles in refrigerant R134a results decrease in COP, which is due to increased viscosity of refrigerant and increased compressor work.

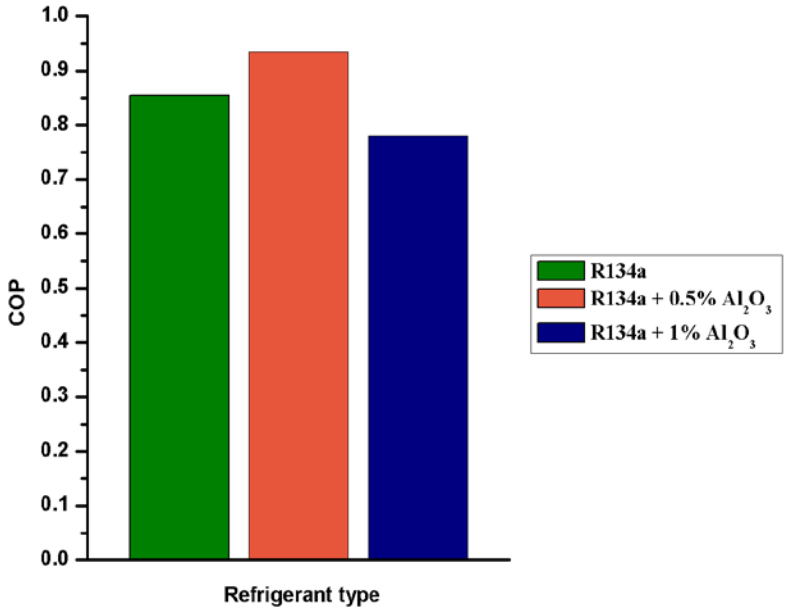

Figure 4.2 – COP comparison for system operating with 6.5 LPH volume flow rate, evaporator load at 15-17^{o}C and at 28^{o}C ±1^{o}C ambient temperature

Now when effect of environment temperature on COP is examined, it has been found that higher ambient temperature results decrease in COP in all three cases. As shown in Figure 4.3 that system works more effectively in lower ambient temperature (21^{o}C ±1^{o}C) with 6.5 LPH volume flow rate and constant evaporator load around 15-17^{o}C. Pure refrigerant R134a at 28^{o}C ±1^{o}C gives 12.26% less COP compared to COP of system operating at 21^{o}C ±1^{o}C ambient temperature. Similarly, nanorefrigerant with 0.5% Al_2O_3 and 1% Al_2O_3 operating at 28^{o}C ±1^{o}C gives 12.25% and 15.95% less COP when compared to COP of system at 21^{o}C ±1^{o}C ambient temperature. This may be due increase in operating temperature of compressor and condenser, which results lower efficiency of both the components.

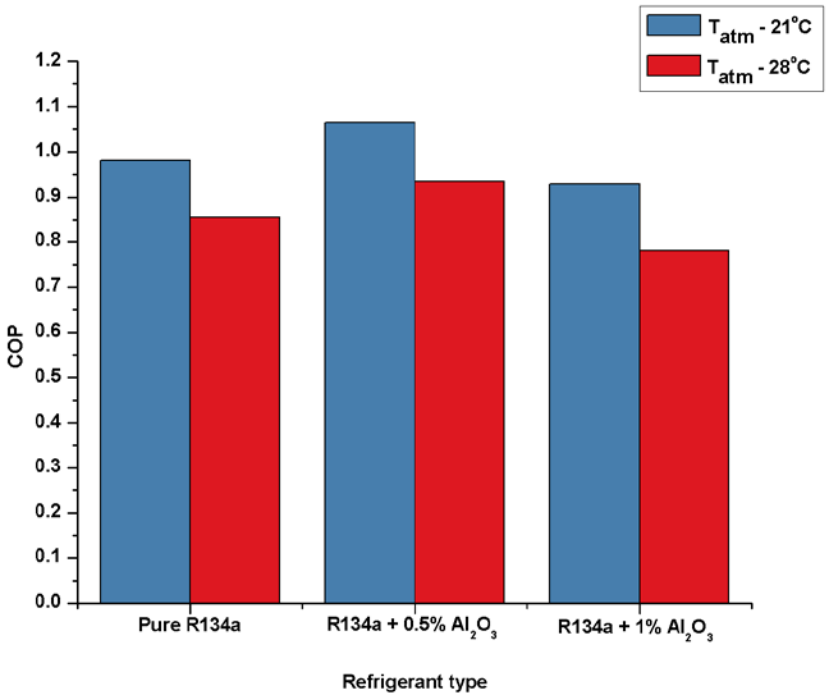

Figure 4.3 – COP comparison for 6.5 LPH volume flow rate, evaporator load at 15-17^{o}C operating at ambient temperature 21 ^{o}C ±1^{o}C and 28 ^{o}C ±1^{o}C

Same experiment is now performed by increasing evaporator load temperature, which is kept constant around 30-31^{o}C, whereas other parameters are kept unchanged like refrigerant volume flow rate 6.5 LPH. As shown in Figure 4.4, at 21 ^{o}C ±1^{o}C ambient temperature, COP with R134a, R134a + 0.5% Al_2O_3 and with R134a + 1% Al_2O_3 is found to be 0.931, 1.011 and 0.889 respectively. So at 0.5% Al_2O_3 in base refrigerant R134a COP get improved by 8.58% and with 1% Al_2O_3 in base refrigerant COP decreases by 4.50% when compared with COP of pure R134a.

Same study is then carried out with 6.5 LPH volume flow rate and 30-31^{o}C evaporator load temperature at 28 ^{o}C ±1^{o}C ambient temperature. As shown in Figure 4.5, with pure R134a, R134a + 0.5% Al_2O_3 and with R134a + 1% Al_2O_3, the COP is in order of 0.909, 0.975 and 0.861 respectively. So with R134a + 0.5% Al_2O_3, COP is found to be enhanced by 7.20% and with 1%

Al_2O_3 particles in base refrigerant COP is found to be decreased by 5.28% as compared to the COP of pure R134a.

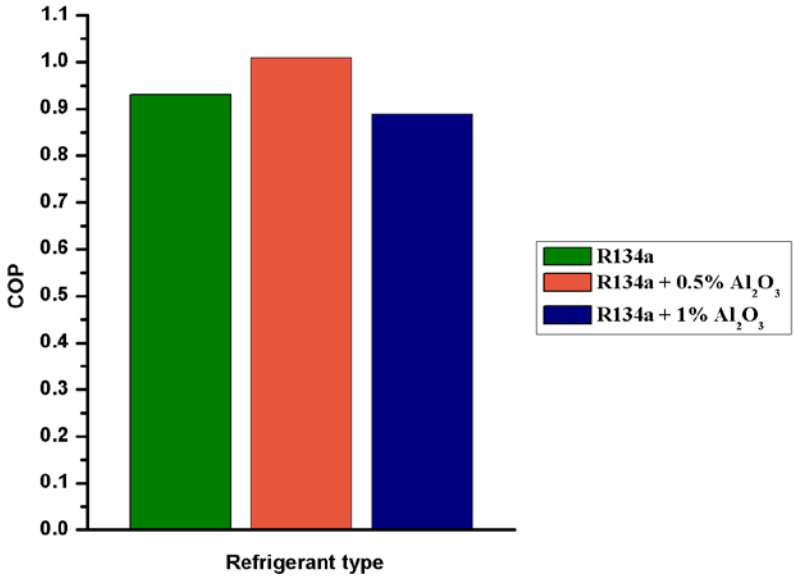

Figure 4.4 – COP comparison for system operating with 6.5 LPH volume flow rate, evaporator load at 30-31^{o}C and at 21^{o}C ±1^{o}C ambient temperature

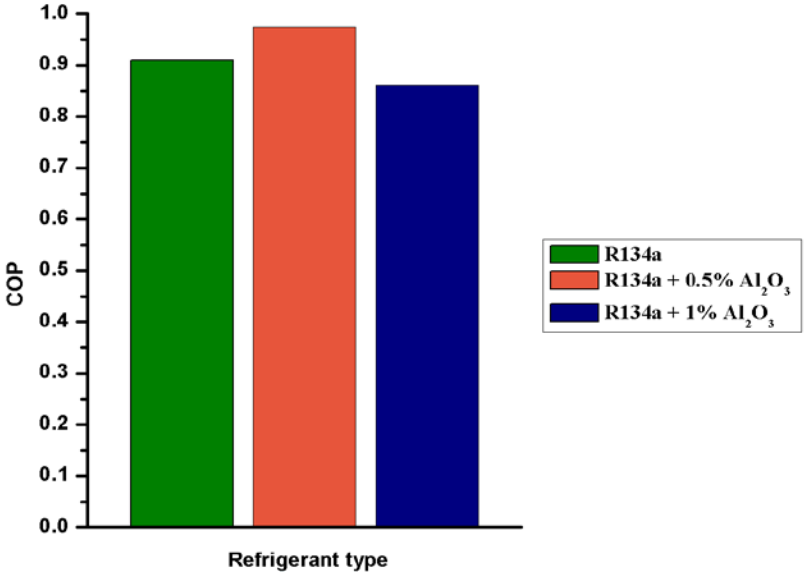

Figure 4.5 – COP comparison for system operating with 6.5 LPH volume flow rate, evaporator load at 30-31^{o}C and at 28^{o}C ±1^{o}C ambient temperature

As shown in Figure 4.6, when effect of environment temperature is studied, it is found that pure R134 operating at 28 ^{o}C ±1^{o}C ambient temperature gives 2.33% less COP than system operating at 21 ^{o}C ±1^{o}C ambient. Whereas R134a + 0.5% Al_2O_3 and R134a + 1% Al_2O_3 operating at 28 ^{o}C ± 1^{o}C ambient gives less COP of the order of 3.57% and 3.13% respectively, when compared to COP for operating ambient temperature 21 ^{o}C ±1^{o}C.

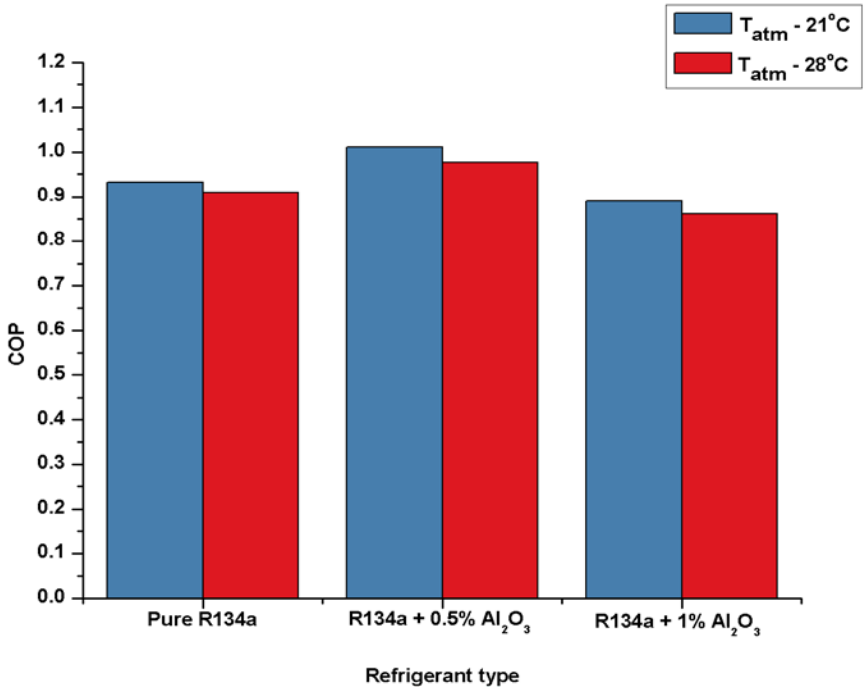

Figure 4.6 – COP comparison for 6.5 LPH volume flow rate, evaporator load at 30-31^{o}C operating at ambient temperature 21 ^{o}C ±1^{o}C and 28±1^{o}C

After above study the flow rate is increased to 11 LPH and in same order COP is studied first at 15-17^{o}C constant evaporator load temperature and ambient temperature around 21 ^{o}C ±1^{o}C. As Figure 4.7 shows, with pure R134a COP is found to be 0.773, whereas with R134a + 0.5% Al_2O_3 and with R134a + 1% Al_2O_3, COP is of order of 0.883 and 0.737 respectively. So with R134a + 0.5% Al_2O_3, COP is found to be improved to around 14.23% and by using R134a + 1% Al_2O_3 COP is found to be decreased to around 4.69%.

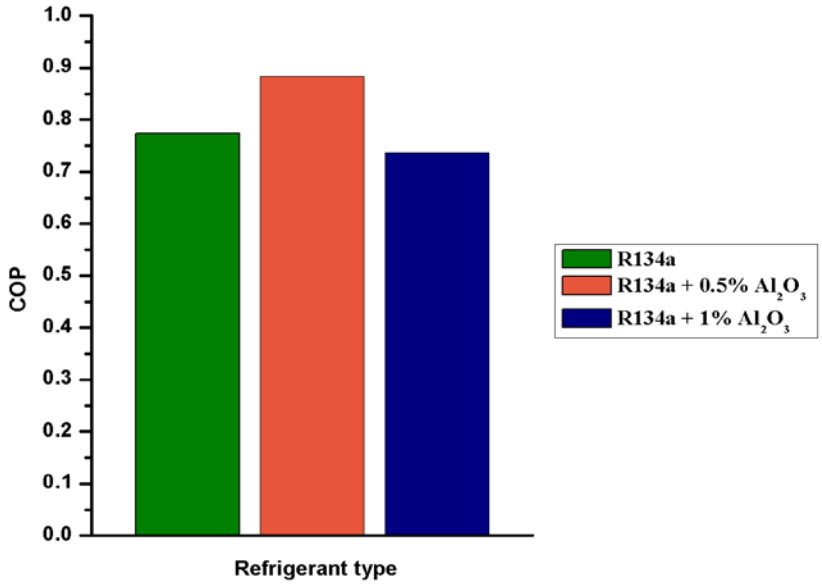

Figure 4.7 – COP comparison for system operating with 11 LPH volume flow rate, evaporator load at 15-17^{o}C and at 21^{o}C±1^{o}C ambient temperature

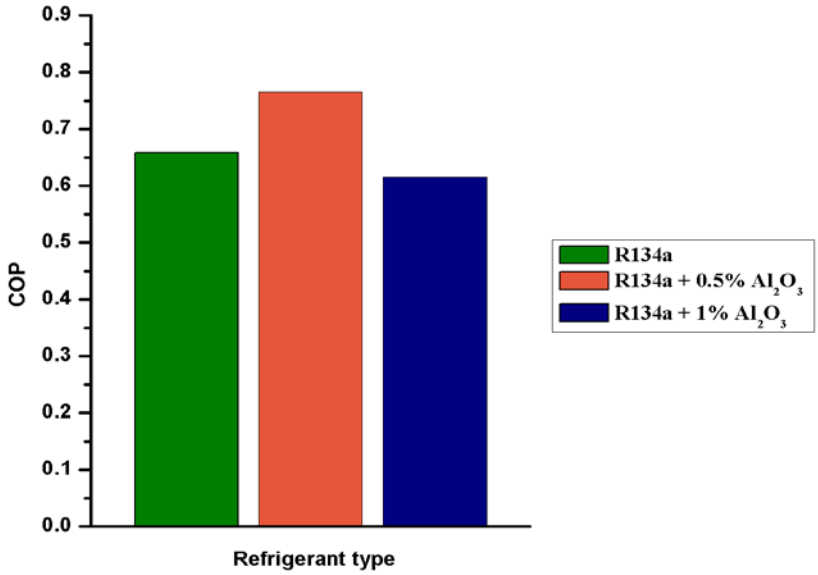

Figure 4.8 – COP comparison for system operating with 11 LPH volume flow rate, evaporator load at 15-17^{o}C and at 28^{o}C±1^{o}C ambient temperature

Now as shown in Figure 4.8 at 28 ^{o}C ±1^{o}C ambient temperature for pure R134a COP is 0.658, further with R134a + 0.5% Al_2O_3 and R134a + 1% Al_2O_3 COP is found of order of 0.766 and

0.615 respectively. So after analysis it has been observed that with R134a + 0.5% Al_2O_3 COP is increased by 16.34% as compared to the COP for pure R134a. Whereas with R134a + 1% Al_2O_3, COP is found to be decreased by 6.49% as compared to COP for pure R134a. Hence same kinds of results have been observed in this case also that at higher mass fraction of Al_2O_3 nanoparticles COP follows decreasing trend.

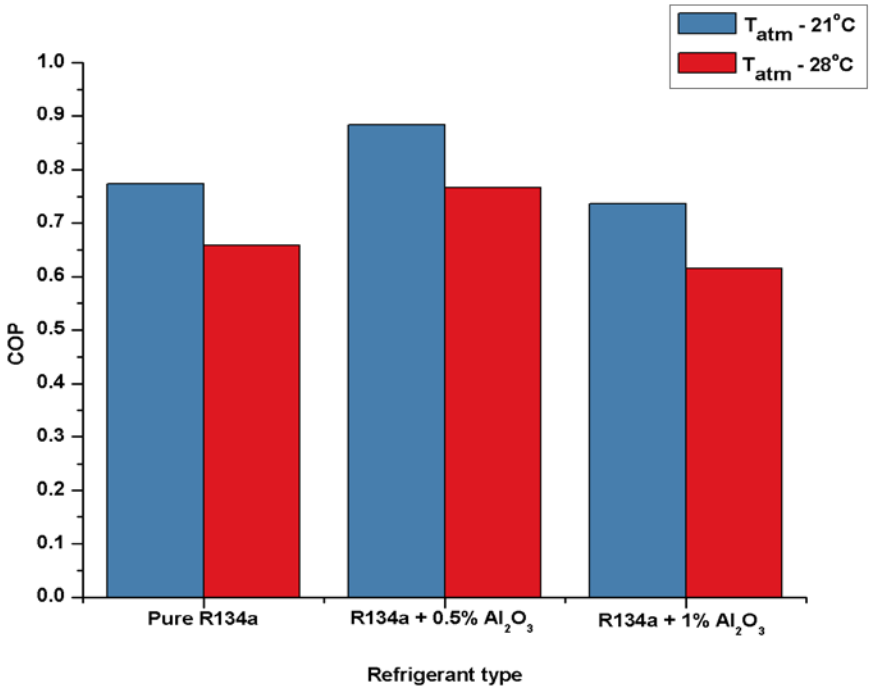

Figure 4.9 – COP comparison for 11 LPH volume flow rate, evaporator load at 15-17^oC operating at ambient temperature 21 ^oC ±1^oC and 28^oC±1^oC

As shown in Figure 4.9, when COP results for 11 LPH refrigerant volume flow rate and constant evaporator load at 15-17^oC at different ambient temperatures are compared, then it has been found that pure R134a at 28^oC±1^oC gives 14.87% less COP as compared to COP of system operating at 21^oC±1^oC ambient temperature. Similarly nanorefrigerant with 0.5% Al_2O_3 and 1% Al_2O_3 operating at 28^oC±1^oC gives 13.30% and 16.48% less COP when compared to COP of system at 21^oC±1^oC ambient temperature.

Now keeping volume flow rate as 11 LPH, same experiment is conducted with constant evaporator heat load 30-31^{o}C. As shown in Figure 4.10, at 21^{o}C±1^{o}C ambient temperature COP with R134a, R134a + 0.5% Al_2O_3 and R134a + 1% Al_2O_3 is found to be 0.853, 0.937 and 0.866 respectively. So 0.5% Al_2O_3 in base refrigerant R134a improves COP to the order of 9.84% and 1% Al_2O_3 in base refrigerant results increase in COP by 1.57% when compared with pure R134a.

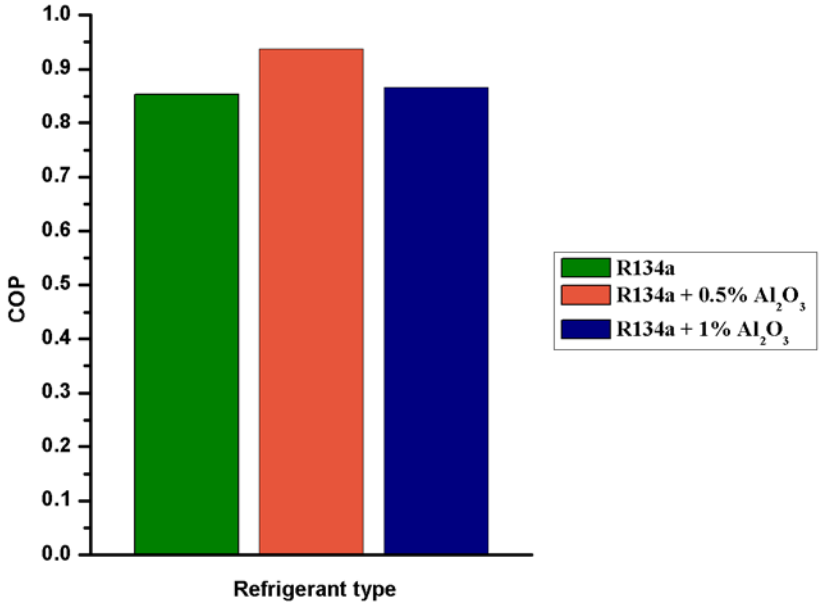

Figure 4.10 – COP comparison for system operating with 11 LPH volume flow rate, evaporator load at 30-31^{o}C and at 21^{o}C±1^{o}C ambient temperature

Then same experiment has been carried out at increased ambient temperature (28^{o}C±1^{o}C) keeping the flow rate as 11 LPH. As shown in Figure 4.11, in this case COPs have been found of order of 0.802, 0.897 and 0.839 for pure R134a, R134a + 0.5% Al_2O_3 and R134a + 1% Al_2O_3 respectively. So in comparison with pure R134a, for 0.5% Al_2O_3 based nanorefrigerant COP increases by 11.87% and refrigerant with 1% Al_2O_3 also gets COP improved by 4.66%. So with higher temperature evaporator load, R134a + 0.5% Al_2O_3 and R134a + 1% Al_2O_3 also shows improvement in COP.

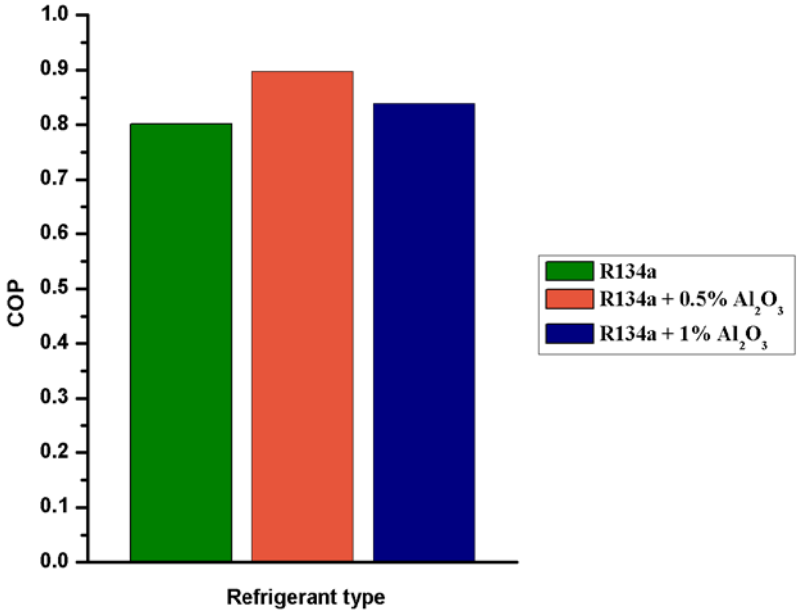

Figure 4.11 – COP comparison for system operating with 11 LPH volume flow rate, evaporator load at 30-31^{o}C and at 28^{o}C±1^{o}C ambient temperature

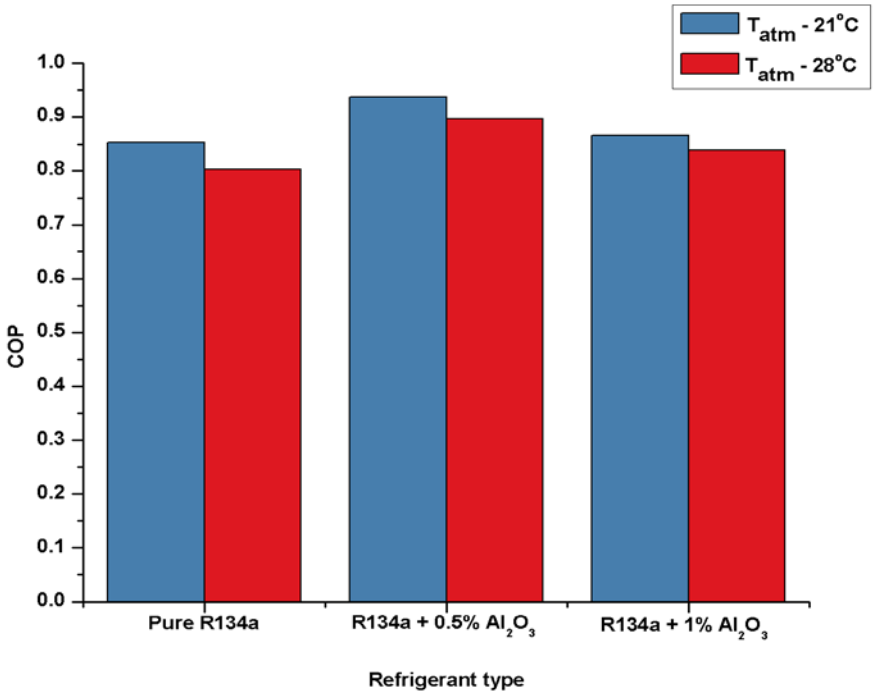

Figure 4.12 – COP comparison for 11 LPH volume flow rate, evaporator load at 30-31^{o}C operating at ambient temperature 21^{o}C ±1^{o}C and 28^{o}C±1^{o}C

As shown in Figure 4.12, when effect of environment temperature is studied, it is found that pure R134a operating at 28 ^{o}C ±1^{o}C ambient temperature gives 5.96% less COP than operating at 21 ^{o}C ±1^{o}C ambient temperature. Whereas R134a + 0.5% Al_2O_3 and R134a + 1% Al_2O_3 operating at 28 ^{o}C ±1^{o}C ambient gives less COP of the order of 4.22% and 3.09% respectively, when compared to operating ambient temperature of 21 ^{o}C ±1^{o}C.

4.2 REFRIGERANT TEMPERATURE DROP ACROSS THE CONDENSER

The condenser is a tube in which refrigerant at high pressure and temperature vapour refrigerant is cooled and condensed at constant pressure. While passing through condenser refrigerant rejects its latent heat to surroundings and change its phase from vapour to liquid. The total heat of hot vapour refrigerant is sum of heat absorbed in evaporator and heat added in compressor. The heat is first transferred to walls of the condenser tubes and then from tubes to cooling medium. In this experimental test rig air is used as cooling medium with natural convection and wire and tube type condenser is used. Sometimes, after condensation process refrigerant is cooled below saturation temperature before expansion. Such process is called subcooling of the refrigerant. The ultimate effect of subcooling is to increase the value of coefficient of performance. In following study temperature drop for refrigerant across the condenser has been studied.

Firstly, temperature drop across the condenser has been studied at 21^{o}C ±1^{o}C ambient temperature, as Figure 4.13 shows that with 6.5 LPH volume flow rate of refrigerant and maintaining constant evaporator load temperature around 15-17^{o}C, the temperature drop across the condenser is 29.87^{o}C for pure R134a. Whereas using R134a + 0.5% Al_2O_3 and R134a + 1% Al_2O_3 nanorefrigerant samples temperature drop across the condenser becomes 31.02^{o}C and 35.23^{o}C respectively. So by using 0.5% Al_2O_3 in base refrigerant a 3.85% more temperature drop

and with 1% Al_2O_3 in base refrigerant around 17.95% more temperature drop is achieved across the condenser as compared to pure R134a. When constant evaporator load is increased to 30-31^oC, maintaining all other parameters unchanged, R134a, R134a + 0.5% Al_2O_3 and R134a + 1% Al_2O_3 gives 34.16^oC, 35.75^oC and 39.38^oC temperature drop across the condenser. So when results for pure R134a refrigerant are compared with nanoparticles based refrigerant samples, it is found that by using R134a + 0.5% Al_2O_3 and R134a + 1% Al_2O_3, a 4.66% and a 15.26% more temperature drop has been achieved across the condenser.

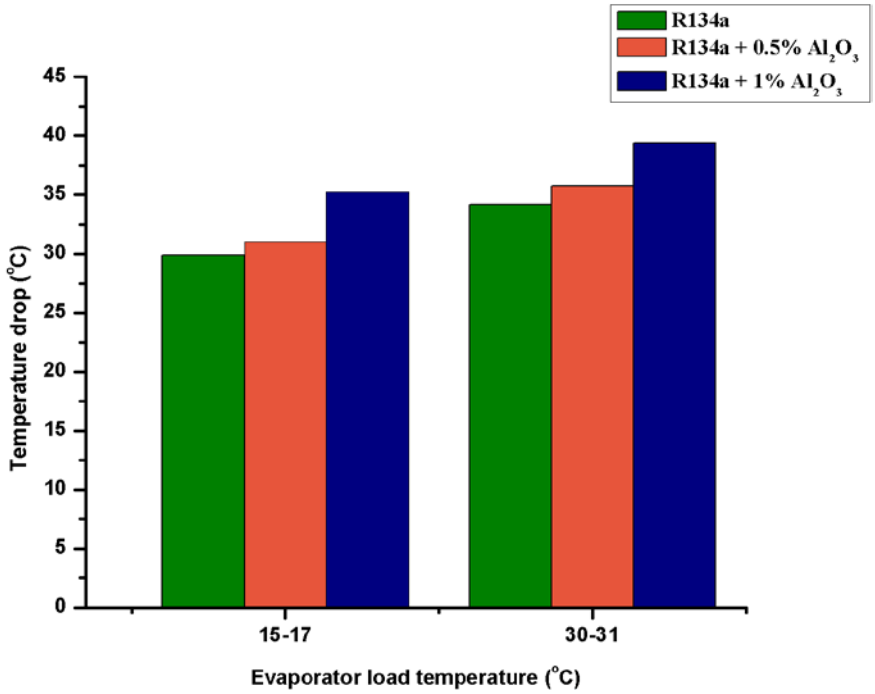

Figure 4.13 – Refrigerant temperature drop across condenser for 6.5 LPH volume flow rate at 21^oC ±1^oC ambient temperature

As Figure 4.14 shows, the temperature drop for 6.5 LPH flow rate at 15-17^oC constant evaporator heat load and where ambient temperature 28^oC ±1^oC, for pure R134a, temperature drop of refrigerant in condenser is 28.89^oC, whereas with R134a + 0.5% Al_2O_3 and R134a + 1% Al_2O_3 drop is 30.21^oC and 34.18^oC respectively. So, 4.55% more temperature drop with 0.5%

Al_2O_3 and 18.31% increase in temperature drop with 1% Al_2O_3 is found as compared to temperature drop in case of pure R134a. Same trend has been observed with 30-31^oC constant evaporator heat load, here temperature drop in condenser is 33.53^oC, 34.91^oC and 38.88^oC for R134a, R134a + 0.5% Al_2O_3 and R134a + 1% Al_2O_3 respectively. Likewise 4.11% and 15.97% more temperature drop with 0.5% Al_2O_3 and 1% Al_2O_3 respectively is observed as compared to pure R134a. So, results shows more temperature drop across the condenser, hence sub-cooling is obtained in condenser, which enhances refrigeration effect of system. This sub cooling is obtained due to improvement in heat transfer characteristics of refrigerant by adding nanoparticles, which results better efficiency of condenser and thereby increases the performance of the system.

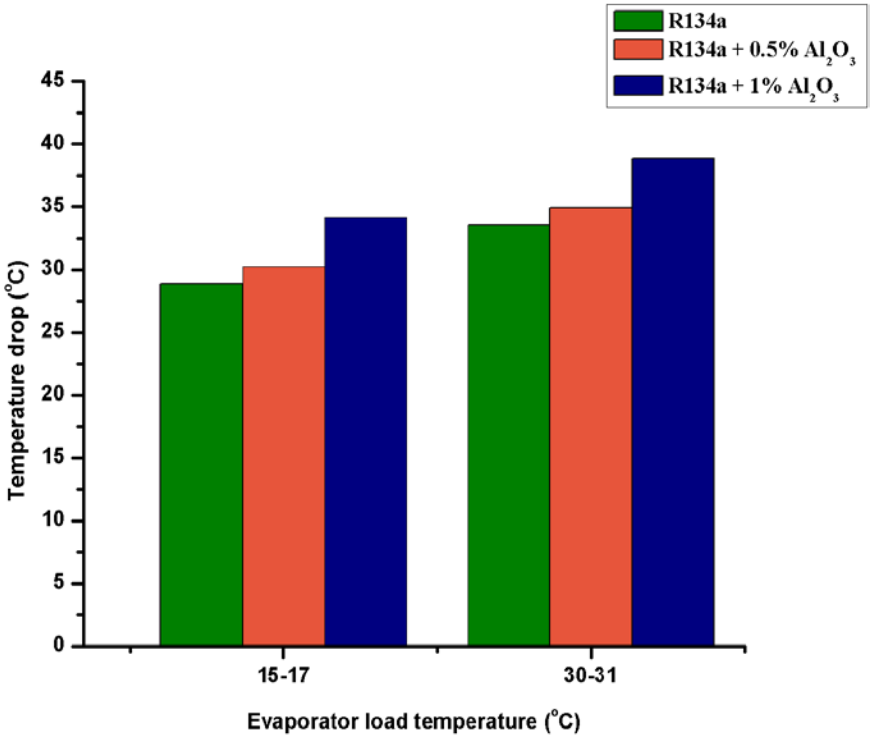

Figure 4.14 – Refrigerant temperature drop across condenser for 6.5 LPH volume flow rate at 28^oC ±1^oC ambient temperature

Now the refrigerant volume flow rate has been increased to 11 LPH. So as Figure 4.15 shows, a temperature drop for 11 LPH flow rate with 15-17^{o}C constant evaporator heat load and ambient temperature 21^{o}C ±1^{o}C, for pure R134a temperature drop of refrigerant in condenser is 28.18^{o}C, whereas with R134a + 0.5% Al_2O_3 and R134a + 1% Al_2O_3 drop is 31.50^{o}C and 36.12^{o}C respectively. So 7.94% more temperature drop with 0.5% Al_2O_3 and 23.77% enhanced temperature drop with 1% Al_2O_3 is observed as compared to pure R134a. After this constant evaporator load has been increased to 30-31^{o}C, while all other parameters remain unchanged, R134a, R134a + 0.5% Al_2O_3 and R134a + 1% Al_2O_3 shows 33.90^{o}C, 34.95^{o}C and 37.95^{o}C temperature drop across the condenser. So when pure R134a refrigerant is compared with nanoparticles based refrigerant samples, it is found that by using R134a + 0.5% Al_2O_3 and R134a + 1% Al_2O_3, a 3.09% and a 11.93% more temperature drop is achieved.

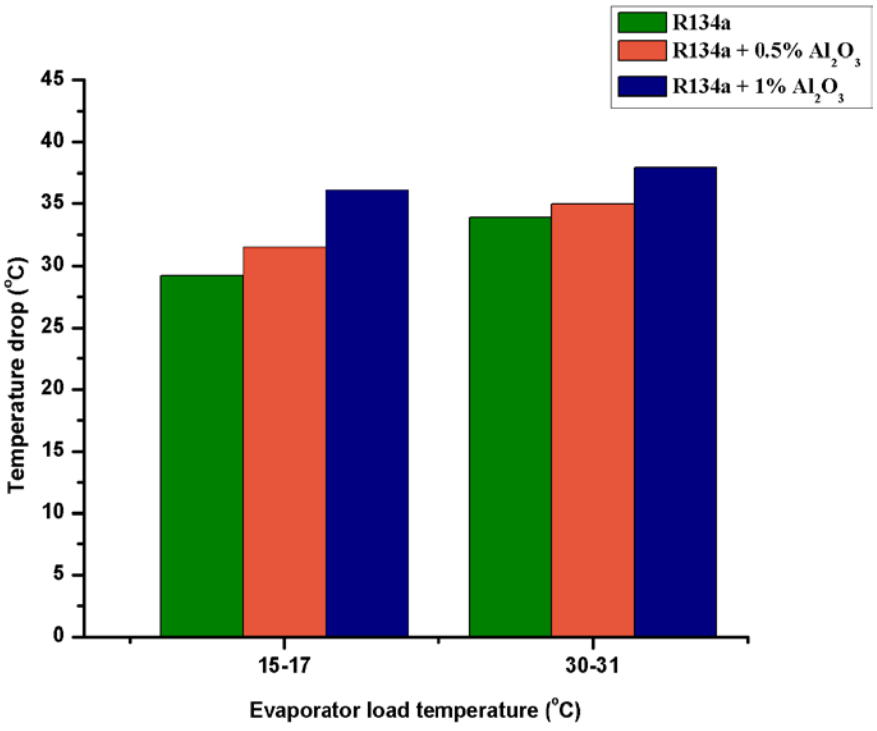

Figure 4.15 – Refrigerant temperature drop across condenser for 11 LPH volume flow rate at 21^{o}C±1^{o}C ambient temperature

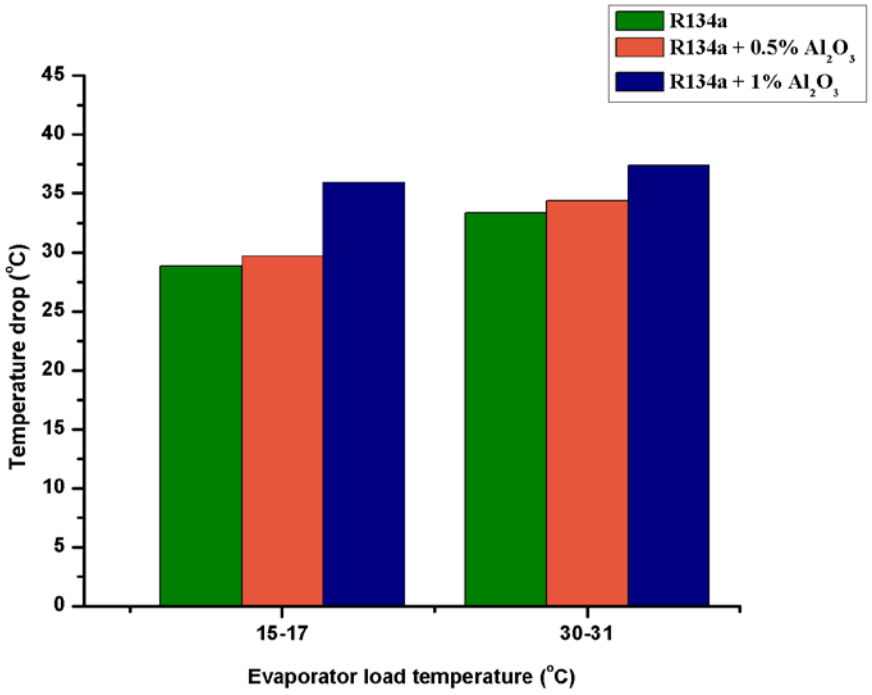

Figure 4.16 – Refrigerant temperature drop across condenser for 11 LPH volume flow rate at 28°C ±1°C ambient temperature

Likewise experimental investigations have also been made at 28°C ±1°C ambient temperature. Figure 4.16 shows a refrigerant temperature drop for 11 LPH flow rate, at 15-17 °C evaporator load, for pure R134a temperature drop across the condenser is 28.87°C, whereas for R134a + 0.5% Al_2O_3 and R134a + 1% Al_2O_3 drop is 29.74°C and 35.96 °C respectively. Hence it is concluded that there is 3.00% more temperature drop with 0.5% Al_2O_3 and 24.55% increase in temperature drop with 1% Al_2O_3 as compared to pure R134a. This all reflect the enhancement in heat transfer characteristics, hence subcooling. When the same study has been conducted with 30-31 °C evaporator load and 11 LPH volume flow rate it is observed that with pure R134a, around 33.25°C temperature drop is achieved across the condenser, whereas with R134a + 0.5% Al_2O_3 and R134a + 1% Al_2O_3 the drop is 34.40 °C and 37.41°C respectively. So there is 3.13% improvement is observed by using 0.5% Al_2O_3 and 12.16% improvement with 1% Al_2O_3 in base

refrigerant R134a as comparison to pure R134a. Hence it has been concluded that by adding Al_2O_3 nanoparticles in refrigerant R134a, the rate of heat transfer in condenser is improved and results subcooling of refrigerant in the condenser.

4.3 REFRIGERANT TEMPERATURE GAIN ACROSS THE EVAPORATOR

After expansion the liquid-vapour mixture enters into the evaporator at low pressure and temperature, where it is evaporates into vapour refrigerant at constant pressure and temperature. During evaporation process refrigerant absorbs its latent heat of vaporization from the medium to be cooled as water in this experiment. This heat absorbed by refrigerant is called refrigerating effect.

Like the condenser experimental investigations have also been made to study the temperature gain across the evaporator. Firstly the refrigerant temperature gain in evaporator has been studied at 21^oC ±1^oC ambient temperature. As Figure 4.17 shows that with 6.5 LPH volume flow rate of refrigerant and by maintaining constant evaporator load temperature around 15-17^oC the temperature gain across the evaporator is 19.63^oC for pure R134a. Whereas using R134a + 0.5% Al_2O_3 and R134a + 1% Al_2O_3 samples temperature drop across the evaporator is found to be 23.87^oC and 27.06^oC respectively. So by using 0.5% Al_2O_3 in base refrigerant 21.57% and with 1% Al_2O_3 in base refrigerant around 37.81% more temperature gain is achieved across the evaporator as compared to temperature gain for pure R134a. Whereas when constant evaporator load is increased to 30-31^oC, maintaining all other parameters unchanged, R134a, R134a + 0.5% Al_2O_3 and R134a + 1% Al_2O_3 gives 36.06^oC, 37.75^oC and 39.56^oC temperature gain across the evaporator. So when pure R134a refrigerant results have been compared with nanoparticles based refrigerant samples, it is found that by using R134a + 0.5% Al_2O_3 and R134a + 1% Al_2O_3, a 4.69% and a 9.72% more temperature gain in the evaporator has been achieved.

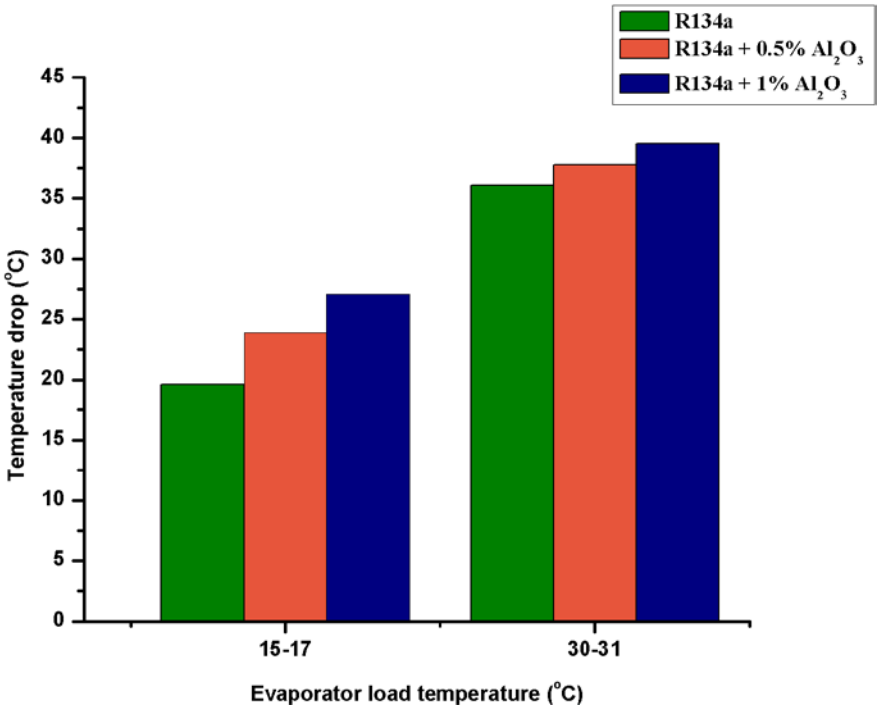

Figure 4.17 – Refrigerant temperature gain across evaporator for 6.5 LPH volume flow rate at 21°C ±1°C ambient temperature

Same trend has been found at 28°C ±1°C ambient temperature, as Figure 4.18 shows that with 6.5 LPH and constant heat load temperature around 15-17°C, the temperature gain across the evaporator is of order of 18.93°C, 22.69 °C and 26.36°C for pure R134a, R134a + 0.5% Al_2O_3 and R134a + 1% Al_2O_3 respectively. It has been observed that there is a 19.87% more gain in temperature across the evaporator for R134a + 0.5% Al_2O_3 and 39.30% more gain with R134a + 1% Al_2O_3 compared to temperature gain in case of pure R134a. Further for same flow rate and 30-31°C constant heat load temperature, the temperature gain of refrigerant across the evaporator is found to be 35.41°C, 37.08 °C and 37.88°C for pure R134a, R134a + 0.5% Al_2O_3 and R134a + 1% Al_2O_3 respectively. So there is 4.72% and 7% more gain in temperature across the evaporator with R134a + 0.5% Al_2O_3 and R134a + 1% Al_2O_3 respectively as compared to temperature gain

with pure R134a. This improvement in temperature gain of refrigerant across the evaporator is due to improved heat transfer properties of the refrigerant flowing through the evaporator.

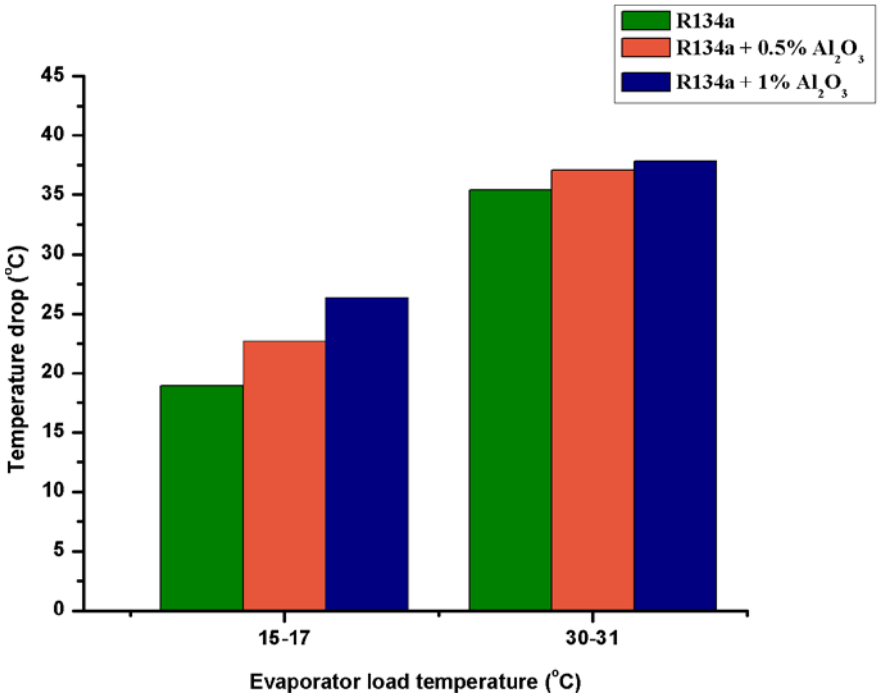

Figure 4.18 – Refrigerant temperature gain across evaporator for 6.5 LPH volume flow rate at 28°C ±1°C ambient temperature

A similar investigation has been done on the refrigerant temperature gain achieved across the evaporator is conducted with 11 LPH refrigerant volume flow rate. As shown in Figure 4.19 with constant heat load temperature around 15-17°C and ambient temperature 21°C±1°C, a gain in temperature across evaporator for R134a, R134a + 0.5% Al_2O_3 and R134a + 1% Al_2O_3 is 18.69°C, 20.27°C and 23.03°C respectively. So when temperature gains, with 0.5% Al_2O_3 and 1% Al_2O_3 samples is compared pure R134a, then a 8.46% and a 23.23% more temperature gain has been observed. Whereas when evaporator heat load temperature has been increased to 30-31°C, keeping all other parameters unchanged, the gain in refrigerant temperature is found to be 29.25°C, 30.96°C and 35.37°C for R134a, R134a + 0.5% Al_2O_3 and R134a + 1% Al_2O_3

respectively. So in comparison to pure R134a, for 0.5% Al_2O_3 based nanorefrigerant there is 5.83% more temperature gain and for nanorefrigerant with 1% Al_2O_3, a 20.93% more refrigerant temperature gain is achieved.

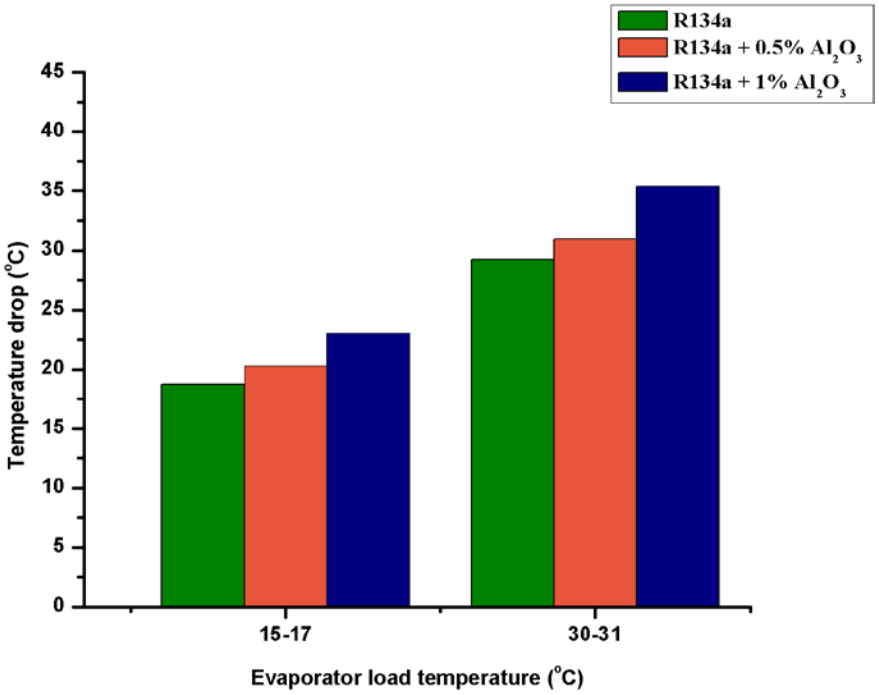

Figure 4.19 – Refrigerant temperature gain across evaporator for 11 LPH volume flow rate at 21°C±1°C ambient temperature

As Figure 4.20 shows, when the same experiment is carried out in 28°C±1°C ambient, with constant evaporator heat load around 15-17°C and keeping refrigerant volume flow rate as 11 LPH, the refrigerant temperature gain across the evaporator is 17.90 °C with pure R134a, whereas with R134a + 0.5% Al_2O_3 and R134a + 1% Al_2O_3 the temperature gain is found to be 19.87°C and 22.25°C respectively. Hence 10.98% and 24.28% improvement has been observed by using 0.5% and 1% nanoparticles in base refrigerant respectively in comparison with pure R134a. Same trend has also been observed with 11 LPH volume flow rate and evaporator load at 30-31°C at same ambient temperature, in this case pure R134a shows 28.68°C temperature gain

across the evaporator, whereas 30.05 ^{o}C and 34.29 ^{o}C temperature gain is obtained by using R134a + 0.5% Al_2O_3 and R134a + 1% Al_2O_3 respectively, which is 4.79% and 19.59%. So from above we can conclude that mixing of Al_2O_3 nanoparticles with refrigerant R134a results improvement in heat transfer characteristics of the nanorefrigerant (R134a + Al_2O_3). Above all it is concluded that the addition of the nanoparticles will increase the effective heat transfer from the medium to be cooled to the refrigerant flowing through the evaporator.

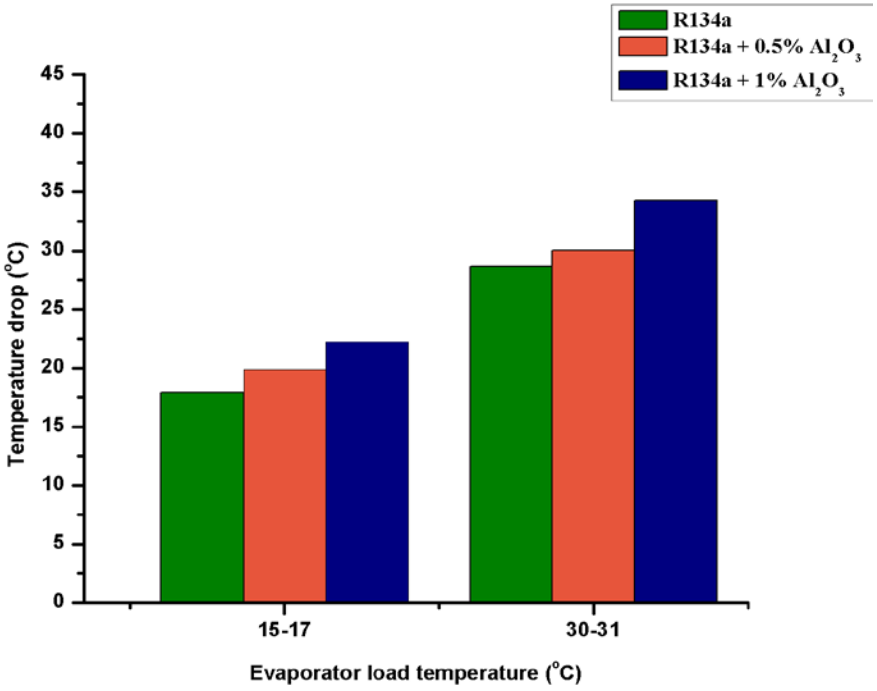

Figure 4.20 – Refrigerant temperature gain across evaporator for 11 LPH volume flow rate at 28^{o}C±1^{o}C ambient temperature

4.4 COOLING LOAD TEMPERATURE - TIME ANALYSIS

An experiment study is conducted to estimate cooling capacity of refrigeration system. First heat is given to load which is water in container around the evaporator coil with the help of heater. The load temperature has been raised to 35^{o}C and then with the help of refrigeration system

temperature is reduced to 8°C and time taken for same has been evaluated at 21°C ±1°C and 28°C ±1°C ambient temperature with 6.5 LPH and 11 LPH refrigerant volume flow rate.

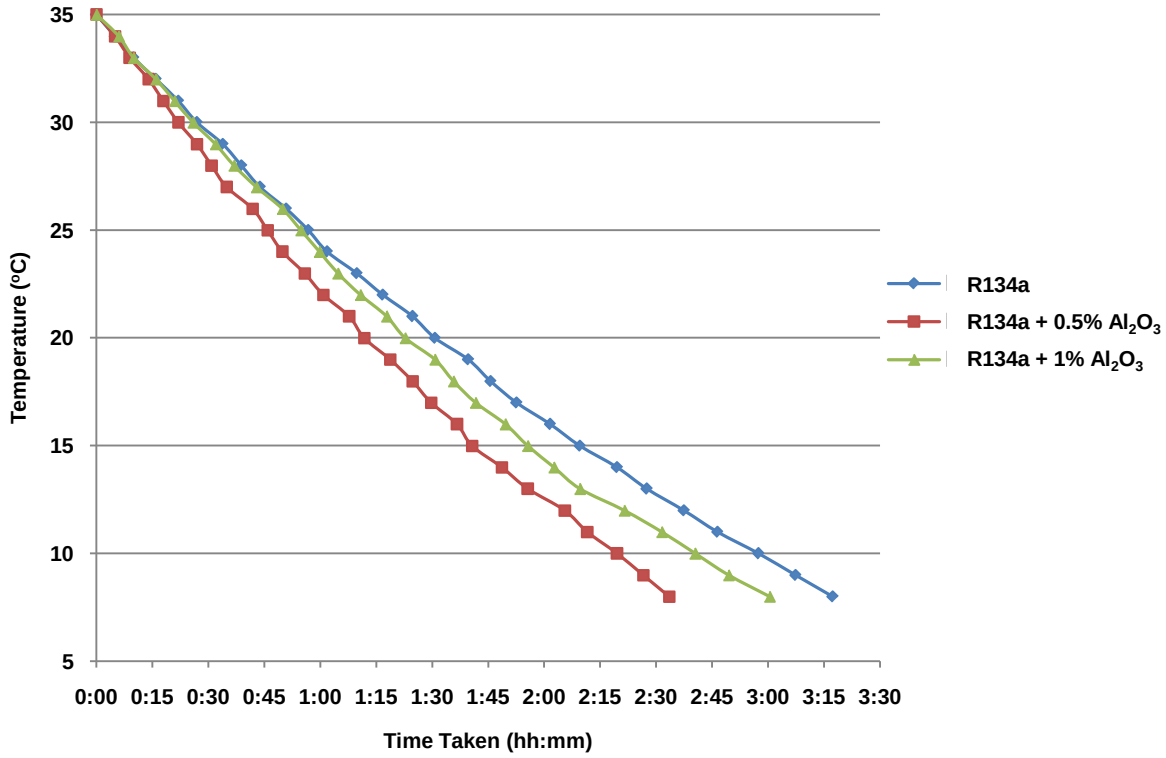

Figure 4.21 – Temperature-time plot for pure R134a and nanorefrigerant R134a + Al_2O_3 operating with 6.5 LPH refrigerant volume flow rate and at 21°C ± 1°C ambient temperature

Figure 4.21 shows the cooling load temperature - time analysis for 6.5 LPH refrigerant volume flow rate at 21°C ±°C ambient temperature. In this study it has been found that pure R134a takes 3 hours 18 minutes for temperature to reduce from 35°C to 8°C, whereas refrigerant R134a with 0.5% Al_2O_3 and 1% Al_2O_3 nanoparticles takes 2 hours 34 minutes and 3 hours and 1 minute to achieve same temperature drop. So results show a 44 minutes and a 17 minutes time saving is achieved with R134a + 0.5% Al_2O_3 and R134a + 1% Al_2O_3 respectively compared to pure R134a. Hence it can be concluded that there is 22.22% and 8.59% less time is taken with 0.5%

Al_2O_3 and 1% Al_2O_3 based nanorefrigerant respectively in comparison with base refrigerant R134a to achieve the same temperature drop in the evaporator.

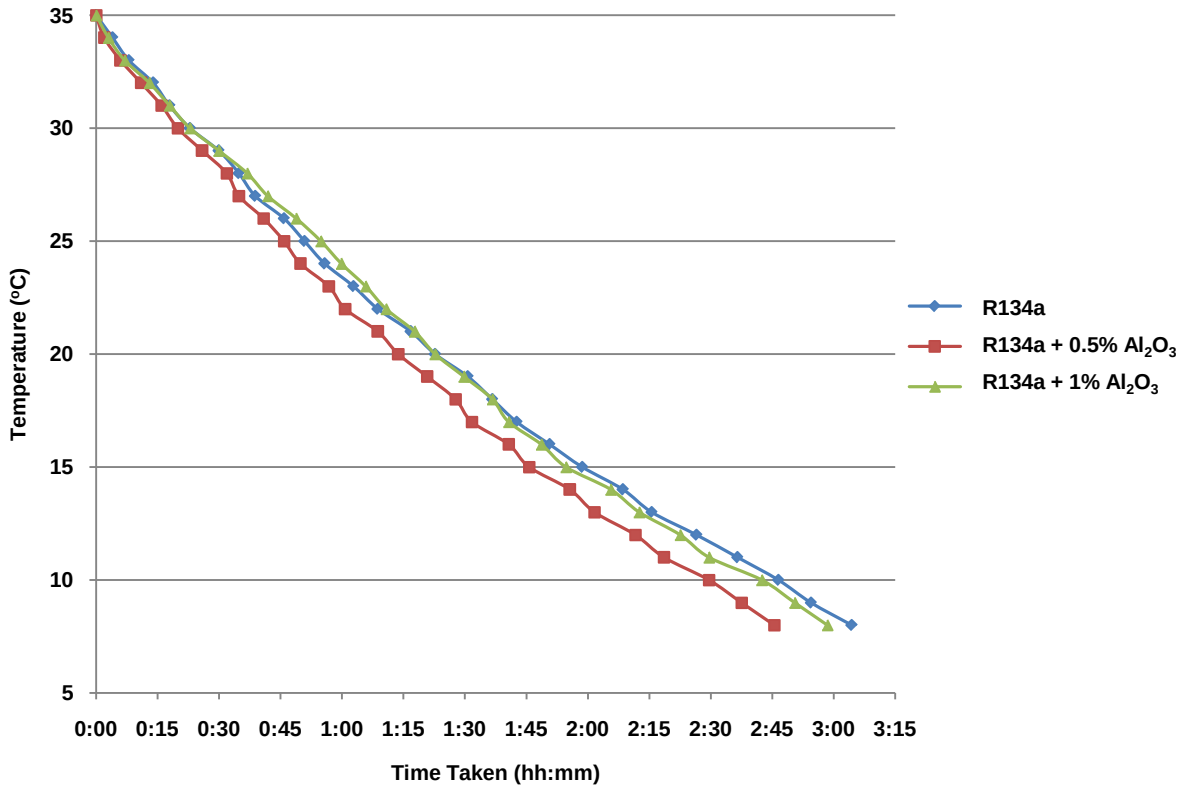

Figure 4.22 – Temperature-time plot for pure R134a and nanorefrigerant R134a + Al_2O_3 operating with 11 LPH refrigerant volume flow rate and at 21°C ± 1°C ambient temperature

Similar trend has been observed with 11 LPH refrigerant volume flow rate at 21°C ± 1°C ambient temperature as shown in Figure 4.22. Investigation shows that pure R134a takes 3 hours 5 minutes for temperature drop from 35°C to 8°C of cooling load, whereas nanorefrigerant with 0.5% Al_2O_3 and 1% Al_2O_3 nanoparticles takes 2 hours 46 minutes and 2 hours 59 minutes respectively for same desired temperature drop. So it is estimated that with R134a + 0.5% Al_2O_3 and R134a + 1% Al_2O_3 there is 19 minutes and 6 minutes time saving respectively, which is 10.27% and 4.79% less than time taken by R134a. But in this case with 11 LPH refrigerant volume flow rate, the time reduction by using Al_2O_3, 20nm nanoparticles is found to be less than

as obtained with 6.5 LPH flow rate. Hence it can be concluded that use of Al_2O_3-20nm nanoparticles in R134a is effective as it improves the heat transfer characteristics of base refrigerant flowing through evaporator, which is due to increased heat carrying capacity of nanofluid (R134a + Al_2O_3). Increased heat carrying capacity is due to higher values of thermal conductivity of the nanorefrigerant. But at same time it is observed that with increase in refrigerant volume flow rate through the evaporator, the cooling time decreases. It may be due to improper expansion of the refrigerant in the system. Further in case of high refrigerant volume flow rate temperature after expansion is also found to be higher than temperature at lower volume flow rates.

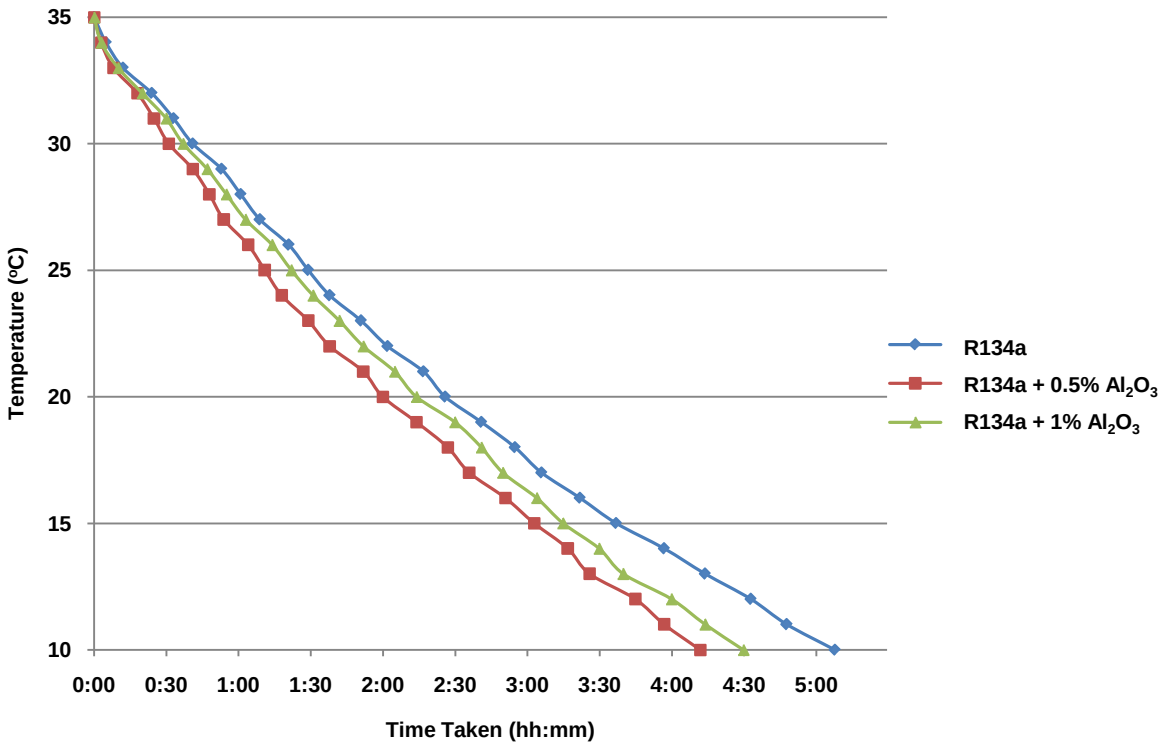

Figure 4.23 – Temperature-time plot for pure R134a and nanorefrigerant R134a + Al_2O_3 operating with 6.5 LPH refrigerant volume flow rate and at 28^{o}C ± 1^{o}C ambient temperature

Likewise, the experiments are carried out at 28°C ± 1°C with 0.5% Al_2O_3 and 1% Al_2O_3 mass fraction in base refrigerant R134a. Initially the study is conducted with 6.5 LPH refrigerant volume flow rate, as shown in Figure 4.23 it is found that with pure R134a time taken to bring down temperature from 35°C to 10°C is around 5 hours 8 minutes, whereas with R134a+0.5% Al_2O_3 and R134a+1% Al_2O_3 based nanorefrigerant time taken is 4 hours 12 minutes and 4 hours 30 minutes respectively. Hence nanorefrigerant with 0.5% Al_2O_3 and 1% Al_2O_3 takes 56 minutes and 38 minutes less than the time taken by the pure R134a, so there is a 18.18% and a 12.34% time saving to achieve a particular temperature (35°C to 10°C).

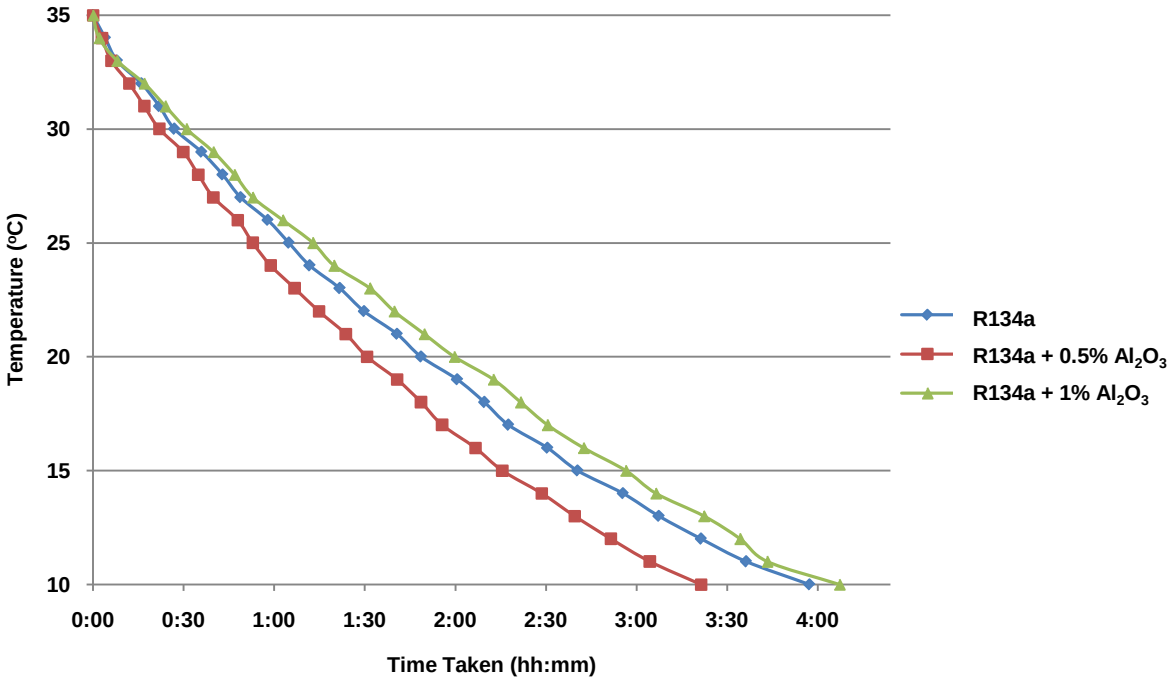

Figure 4.24 – Temperature-time plot for pure R134a and nanorefrigerant R134a + Al_2O_3 operating with 11 LPH refrigerant volume flow rate and at 28°C ± 1°C ambient temperature

But when same experiment is carried out with 11 LPH volume flow rate at 28°C ± 1°C atmospheric temperature as shown in Figure 4.24, it has been analyzed that the nanorefrigerant

with 1% Al_2O_3 mass fraction takes more time as compared to pure R134a for temperature reduction from 35^oC to 10^oC of evaporator load. As shown in Figure 4.24 pure refrigerant R134a takes 3 hours 58 minutes whereas nanorefrigerant with 0.5% Al_2O_3 and 1% Al_2O_3 takes 3 hours 22 minutes and 4 hours 8 minutes respectively to achieve the desired temperature drop from 35^oC to 10^oC. So, R134a + 0.5% Al_2O_3 takes 36 minutes less and R134a + 1% Al_2O_3 takes 10 minutes more than the time taken by pure R134a to achieve desired temperature drop of 35^oC to 10^oC. This shows a 15.13% time reduction with R134a + 0.5% Al_2O_3, but R134a + 1% Al_2O_3 takes a 4.20% more time than R134a to achieve same temperature drop.

So from this it can be concluded that Al_2O_3 (20nm) nanoparticles in refrigerant R134a show an improvement in refrigerating capacity of vapour compression system which is due to increased heat carrying capacity of nanoparticles based refrigerant. But at higher mass fractions and at higher refrigerant volume flow rates, it may also decrease in refrigeration capacity compared to R134a, this may be due to improper evaporation and expansion. Also with increase in ambient temperature the improvement is decreasing which is due to increased losses to environment and higher condenser operating temperature.

4.5 POWER CONSUMPTION

Power input to any refrigeration system is an important parameter to evaluate its performance and COP of refrigeration system depends on it. In earlier experiments it has been found that the addition of Al_2O_3, 20nm nanoparticles upto 1% (by weight) decreases the time taken in the evaporator space to achieve a particular temperature, hence there is an improvement in refrigeration capacity. But along with this, what is its effect on the power consumption of the system is also a matter of concern. In this section the power requirements to run the system has been examined to achieve desired temperature as discussed in previous section.

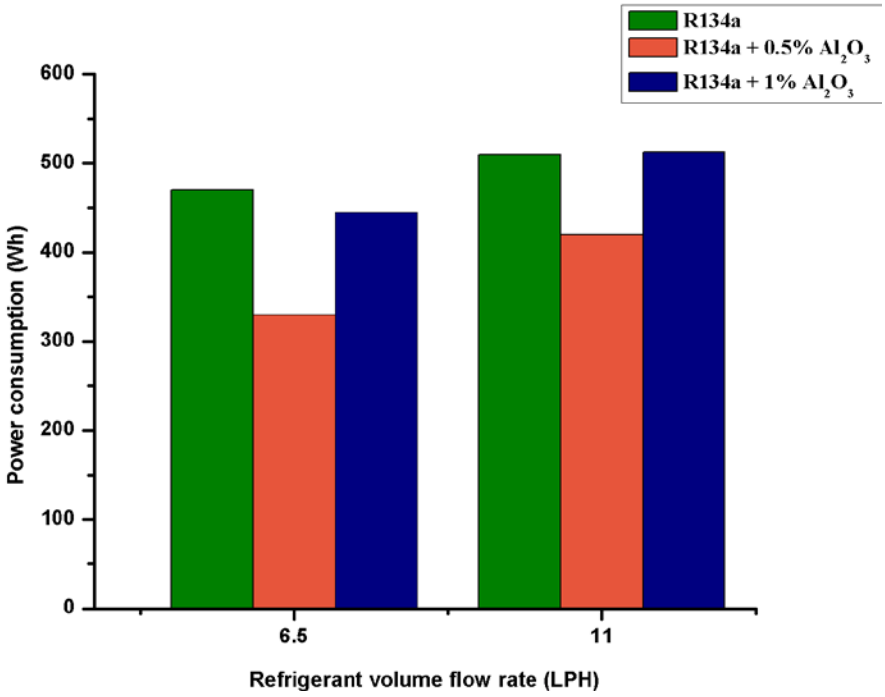

Figure 4.25 – Power consumption for temperature drop (35^{o}C to 8^{o}C) in evaporator for pure R134a and nanorefrigerant R134a + Al_2O_3 operating with 6.5 LPH and 11 LPH refrigerant volume flow rate and at 21^{o}C ± 1^{o}C ambient temperature

As shown in Figure 4.25 it has been found that with 6.5 LPH refrigerant volume flow rate at 21^{o}C ± 1^{o}C ambient temperature, there is a 29.79% and 5.32% reduction in power consumption with R134a + 0.5% Al_2O_3 and R134a + 1% Al_2O_3 nanorefrigerant as compared to pure R134a for temperature reduction from 35^{o}C to 8^{o}C. It has been examined that pure refrigerant consumes around 470 Wh power whereas 0.5% Al_2O_3 and 1% Al_2O_3 in base refrigerant R134a takes 330 Wh and 445 Wh power respectively. Whereas, when the refrigerant volume flow rate is increased to 11 LPH keeping all other parameters unchanged, it has been found that R134a + 0.5% Al_2O_3 consumes 17.65% less power but R134a + 1% Al_2O_3 consumes 0.59% more power than power consumption for pure R134a. In this case pure R134a consumes 510 Wh power as compared to 420 Wh and 513 Wh power consumption by 0.5% Al_2O_3 and 1% Al_2O_3 in

refrigerant R134a. This has been experimented for same temperature drop in evaporation space (35^oC to 8^oC).

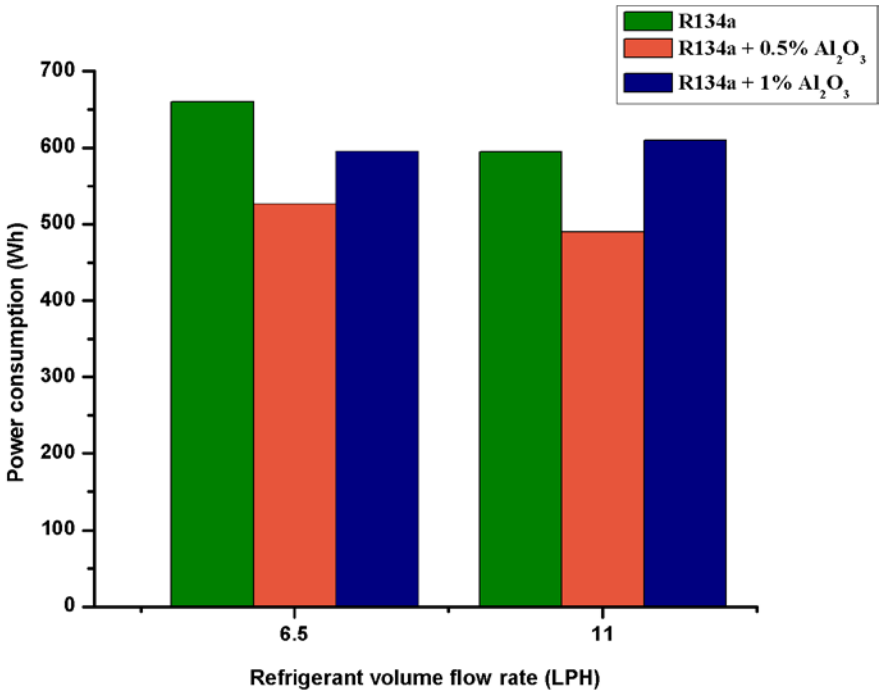

Figure 4.26 – Power consumption for temperature drop (35^oC to 10^oC) in evaporator for pure R134a and nanorefrigerant R134a + Al_2O_3 operating with 6.5 LPH and 11 LPH refrigerant volume flow rate and at $28^oC \pm 1^oC$ ambient temperature

Similar study has been carried out at higher ambient temperature ($28^oC\pm 1^oC$), as shown in Figure 4.26. In this study it has been found that at 6.5 LPH refrigerant volume flow rate, a pure R134a, R134a + 0.5% Al_2O_3 and R134a + 1% Al_2O_3 consumes 660 Wh, 527 Wh and 596 Wh respectively to reduce refrigeration space temperature from 35^oC to 10^oC. So 0.5% Al_2O_3 and 1% Al_2O_3 nanoparticles in base refrigerant R134a shows 20.15% and 9.70% reduction in power as compared to pure R134a. But when the same experiment has been carried out at 11 LPH refrigerant volume flow rate then it is found that pur`e R134a consumes 595 Wh power, whereas R134a + 0.5% Al_2O_3 and R134a + 1% Al_2O_3 consumes 490 Wh and 610 Wh power respectively.

This is done to achieve a temperature drop from 35^{o}C to 10^{o}C of water (load) around the evaporator. So in this case 0.5% Al_2O_3 nanoparticles in base refrigerant (R134a) takes 17.65% less power whereas 1% Al_2O_3 in R134a results 2.52% more power consumption than pure refrigerant.

So it can be concluded that at both ambient temperatures (21^{o}C ± 1^{o}C and 28^{o}C ± 1^{o}C), if 0.5% Al_2O_3 nanoparticles of 20nm size has been added to R134a, it results in less power consumption of compressor at 6.5 LPH and 11 LPH refrigerant volume flow rates. But 1% Al_2O_3 in base refrigerant R134a shows an improvement i.e. results less power consumption at 6.5 LPH refrigerant volume flow rate, but it takes more power when refrigerant volume flow rate is increased to 11 LPH.

CHAPTER - 5

CONCLUSION AND FUTURE SCOPE

5.1 CONCLUSION

In this study the performance of domestic refrigerator based experimental test setup has been investigated by using pure refrigerant R134 and nanorefrigerant (R134a + Al_2O_3). Experimental facility is developed in our laboratory. Results show that the use of nanorefrigerant (R134a + Al_2O_3) instead of pure refrigerant R134a is advantageous. It has been observed that there is a significant improvement in the performance of the system when nanoparticles are used along with conventional refrigerant (R134a) within certain limit. Following conclusions are derived from this experimental study:-

(i) Coefficient of performance (COP) of vapour compression system is found to be improved by dispersing Al_2O_3 nanoparticles in R134a refrigerant. This improvement is maximum (7.20% to 16.34%) with 0.5% mass fraction of Al_2O_3 in refrigerant for all volume flow rates and evaporator heat fluxes. However 1% Al_2O_3 (by weight) in refrigerant results decrease in COP of the system at all refrigerant volume flow rates and also at lower evaporator heat fluxes. But at higher refrigerant volume flow rate (11 LPH) and higher evaporator heat flux (at 30-31^oC) the COP is found to be enhanced marginally.

(ii) The coefficient of performance (COP) of vapour compression system is found to be decreasing with increase in ambient temperature (from 21^oC to 28^oC) for both pure refrigerant and nanorefrigerant, hence system operates more efficiently at lower ambient temperatures.

(iii) The refrigerant temperature drop across the condenser gets improved (3.00% to 23.77%) by using R134a based nanorefrigerant with Al_2O_3 nanoparticles. This results in subcooling of nanorefrigerant before leaving the condenser. This is due to improved heat transfer characteristics of nanorefrigerant over the conventional refrigerant. The temperature drop increases with increase in Al_2O_3 in refrigerant (R134a).

(iv) The temperature gain across the evaporator is also found to be enhanced (4.69% to 39.30%) by using nanorefrigerant, which is due to improved heat transfer properties. With increase in mass fraction of Al_2O_3 in base refrigerant, the temperature gain in evaporator also increases.

(v) The cooling capacity (time required to achieve a desired temperature) of refrigeration system gets improved by using nanorefrigerant at lower ambient temperatures (21^oC). But at higher ambient temperature (28^oC), it is found that the cooling capacity improves with lower refrigerant volume flow rate (6.5 LPH) but with increase in flow rate (11 LPH) cooling capacity decreases.

(vi) This improved cooling capacity also results in lower power requirements (5.32% to 29.79%), but power requirements increases for higher volume flow rate (11 LPH) at all ambient temperatures.

(vii) The use of 0.5% Al_2O_3 (by weight) in refrigerant R134a improves the system performance, but when the dispersion is increased to 1% the performance of the system is found to be decreased except at higher flow rate (11 LPH) and higher evaporator heat (at $30\text{-}31^oC$) flux where performance improves marginally.

(viii) System works normally with nanorefrigerant.

So from above conclusions it can be concluded that the use of R134a based nanofluid with 0.5% Al_2O_3 is beneficial in order to improve system performance and heat transfer characteristics.

Further the system size can be decreased for same cooling capacity with reduced power requirements. However the performance in long run is point of attention and requires further research.

5.2 CHALLENGES WITH NANOFLUIDS

The use of nanofluids in wide variety of applications appears promising. But the development in this field is hindered by certain points that include lack of agreement on results presented by various researchers, lack of theoretical appreciation of the reasons responsible for properties enhancement. Therefore, there are certain important issues that may receive greater attention in near future. Some major challenges includes:-

(i) Long term stability of nanoparticles dispersion - Preparation of homogeneous nanofluid remains a challenge as the nanoparticles always form clusters due to very strong interactions. However to have stable suspensions, some physical and chemical methods have been introduced that include use of surfactant, modification of particle surface or apply strong opposite forces on suspended particles. Further the heat exchanger operates under laminar conditions, the use of nanofluids is found effective, but at same time high price and instability potential are also requires attention. Moreover, the long term stability of nanoparticles in base fluid is one of the very basic requirements of nanofluids applications. Despite to other common base fluids like ethylene glycol and water, the rapid agglomeration and settling of common nanoparticles has been found in refrigerants.

(ii) Higher viscosity - The viscosity of nanofluids normally increasing with increase particle concentration. In some investigations it has been reported that the nanofluid viscosity increasing rapidly with increase volume percentages of nanoparticles. The increased viscosity consumes more power to run the system.

(iii) Lower specific heat - Some investigations also found that nanofluids specific heat is lower than base fluid. It has been presented that ethylene glycol + CuO, ethylene glycol + SiO_2 nanofluids and ethylene glycol + Al_2O_3 nanofluids have lower specific heat as compared to base fluids [35].

An ideal refrigerant should always possess high specific heat in order to remove more heat from refrigerating space.

(iv) High cost of Nanofluids - Higher cost of production of nanofluids is among the main reasons that restrict their application in industry. Nanofluids can be produced by either one-step or two-step methods and both methods require sophisticated and advanced instruments. Hence high cost associated with nanofluids is also one of the major implications for its applications.

(v) Fouling - Although many nanofluids have been applied with single phase heat transfer application are found effective with enhancement in heat transfer characteristics. But when nanoparticles were applied in the boiling heat transfer applications, it has been pointed out that they caused fouling on heat transfer surface, hence result decrease in the heat transfer coefficient. [35]

5.3 FUTURE SCOPE

The results show that nanofluids have notable potential to improve heat transfer characteristics of refrigerant. However, it is unclear why there significant increase in heat transfer properties is observed with insignificant pressure increase. Moreover, challenges with particle circulation, dispersion and its effects on the compressor of refrigeration system have not been addressed. However, the present investigations are compelling that the further research should be undertaken. Future research is required to investigate the influence of the particle material, size, shape and concentration on refrigerant boiling performance, long term stability of nanoparticles in refrigerant and effect of nanoparticles on various components of refrigeration system. Experimental results on the fundamental properties such as specific heat, density and viscosity of nanorefrigerants are limited in the literatures, so there are potentials to explore research to determine these properties experimentally also.

REFERENCES

[1] Das, S. K., Choi, S.U., Yu, W. and Pradeep, T. (2007), Nanofluids: Science and technology, *Willey Publications*, ISBN: 978-0-470-07473-2.

[2] Yu, W. and Xie, H. (2011), A review on nanofluids: Preparation, stability mechanisms, and applications, *Journal of Nanomaterials*, Vol. 2012, Article ID 435873.

[3] Hwang, Y., Lee, J.K., Jeong, Y.M., Cheong, S.I., Ahn, Y.C. and Kim, S.H. (2008), Production and dispersion stability of nanoparticles in nanofluids, *Powder Technology*, Vol. 186, Issue 2, pp.145–153.

[4] Ghadimi, A., Saidur, R. and Metselaar , H.S.C. (2011), A review of nanofluid stability properties and characterization in stationary conditions, *International Journal of Heat and Mass Transfer*, Vol. 54, pp. 4051–4068.

[5] Saidura, R., Leongb, K.Y., Mohammadc, H.A. (2011), A review on applications and challenges of nanofluids, *Renewable and Sustainable Energy Reviews*, Vol. 15, pp. 1646–1668.

[6] Park, K.J. and Jung, D.S. (2007), Boiling heat transfer enhancement with carbon nanotubes for refrigerants used in building air conditioning, *Energy and Buildings*, 39(9):1061–4.

[7] Trisaksri, V. and Wongwises, S. (2009), Nucleate pool boiling heat transfer of TiO_2–R141b nanofluids, *International Journal of Heat and Mass Transfer*, 52(5–6):1582–8.

[8] Hao, P., Guoliang, D., Weiting, J., Haitao, H. and Yifeng, G. (2009), Heat transfer characteristics of refrigerant-based nanofluid flow boiling inside a horizontal smooth tube, *International Journal of Refrigeration*, 32:1259–70.

[9] Hao, P., Guoliang, D., Haitao, H., Weiting, J., Dawei, Z. and Kaijiang, W. (2010), Nucleate pool boiling heat transfer characteristics of refrigerant/oil mixture with diamond nanoparticles, *International Journal of refrigeration,* 33:347–58.

[10] Coumaressin, T. and Palaniradja, K. (2014), Performance analysis of a refrigeration system using nanofluid, *International Journal of Advanced Mechanical Engineering,* ISSN 2250-3234 Vol. 4, Number 4, pp. 459-470.

[11] Kedzierski, M.A. and Gong, M. (2009), Effect of CuO nanolubricant on R134a pool boiling heat transfer with extensive measurement and analysis details. *USA: NISTIR 7454, National Institute of Standards and Technology*.

[12] Bi, S., Shi L. and Zhang L. (2008), Application of nanoparticles in domestic refrigerators, *Applied Thermal Engineering,* Vol. 28, pp.1834-1843.

[13] Jwo, C.S., Jeng, L.Y., Teng, T.P. and Chang, H. (2009), Effect of nano lubricant on the performance of Hydrocarbon refrigerant system, *J. Vac. Sci. Techno.,* Vol.27, Issue 3, pp. 1473-1477.

[14] Subramani, N. and Prakash, M. J., (2011), Experimental studies on a vapour compression system using nanorefrigerants, *International Journal of Engineering, Science and Technology*, Vol. 3, Issue 9, pp. 95-102.

[15] Kumar, S.D. and Elansezhian, R. (2012), Experimental study on Al_2O_3-R134a nano refrigerant in refrigeration system, *International Journal of Modern Engineering Research,* Vol. 2, Issue. 5, pp. 3927-3929.

[16] Hafez E.A., Taher, S.H., Torki, A.H.M. and Hamad, S.S. (2011), Heat transfer analysis of vapor compression system using nano Cuo-R134a, *International Conference on Advanced Materials Engineering IPCSIT,* Vol.15.

[17] Bi, S., Guo, K., Liu, Z. and Wu, J. (2011), Performance of a domestic refrigerator using TiO_2-R600a nano-refrigerant as working fluid, *Energy Conversion and Management,* Vol. 52, pp. 733–737.

[18] Loaiza, J.C.V., Pruzaesky, F.C. and Parise, J.A.R. (2010), Numerical study on the application of nanofluids in refrigeration systems, *International Refrigeration and Air Conditioning Conference.* Paper 1145.

[19] Sabareesh, R.K., Gobinath, N., Sajith, V., Das, S., Sobhan, C.B. (2012), Application of TiO_2 nanoparticles as a lubricant-additive for vapor compression refrigeration systems - An experimental investigation, *International Journal of Refrigeration*, 35, pp. 1989 – 1996.

[20] Kumar, R.R., Sridhar, K. and Narasimha, M. (2013), Heat transfer enhancement in domestic refrigerator using R600a/mineral oil/nano-Al_2O_3 as working fluid, *International Journal of Computational Engineering Research,* Vol. 3 Issue 4, pp 42-50

[21] Clancy, E.V. (2012), Patent application title: Apparatus and method of using Nanofluids to improve energy efficiency of vapor compression systems, *Patent Application Number: 20120017614.*

[22] Mahbubul, I.M., Saidur, R. and Amalina, M.A. (2011), Pressure drop characteristics of TIO_2–R123 nanorefrigerant in a circular tube, *Engineering e-Transaction (ISSN 1823-6379),* Vol. 6, Issue 2, pp. 124-130.

[23] Peng, H., Ding, G., Jiang, W., Hu, H., Gao Y. (2009), Measurement and correlation of frictional pressure drop of refrigerant-based nanofluid flow boiling inside a horizontal smooth tube, *International Journal of Refrigeration*, 32, pp. 1756‑64.

[24] Kedzierski, M. A. (2013), Viscosity and density of aluminium oxide nanolubricant, *International Journal of Refrigeration*, 36, pp. 1333 – 1340.

[25] Parise, J., Tiecher, R. F. (2012), A Simulation model for the application of nanofluids as condenser coolants in vapor compression heat pumps, *International Refrigeration and Air Conditioning Conference at Purdue*, pp. 2531.

[26] Peng, H., Ding, G., Hu, H., Jiang, W., Zhuang, D. (2010), Nucleate pool boiling heat transfer characteristics of refrigerant/oil mixture with diamond nano particles, *International Journal of Refrigeration*, Vol.33, pp. 347-358.

[27] http://en.wikipedia.org/wiki/1,1,1,2-Tetrafluoroethane

[28] Bi, S., Shi L. and Zhang, L., (2007), Performance study of a domestic refrigerator using R134a/mineral oil/nano-TiO_2 as working fluid, *ICR07-B2-346.*

[29] http://en.wikipedia.org/wiki/X-ray_Diffraction

[30] http://en.wikipedia.org/wiki/Transmissiom_electron_microscopy

[31] http://www.e-refrigeration.com/learn-refrigeration/refrigeration-repairs/using-flare-fittings

[32] Kalpakjian, S. (2013), Manufacturing and engineering technology, *Prentice Hall Publications.*

[33] Groover, Mikell P. (2007), Fundamentals of modern manufacturing, *Materials Processes, And Systems (2nd ed.).* pp. 746-748.

[34] Pawel, K.P., Jeffrey, A.E. and David G.C. (2005), Nanofluids for thermal transport, *Materials Today*, pp. 36-44.

[35] Praveen, K., Namburu, DK., Das, KM. and Ravikanth SV. (2009), Numerical study of turbulent flow and heat transfer characteristics of nanofluids considering variable properties, *International Journal of Thermal Sciences*, 48:290–302.

APPENDIX

S. No.	Description of Item	Qty.	Estimate (in Rs.)	Actual Cost (purchased till now) (in Rs.)	Remarks
1	Al_2O_3 Nanopowder 20nm	20gm	7500	6500	
2	Rotameter	1	3500	4050	-
4	Compressor	1	2500	2500	-
5	Board	1	2000	-	Available in RAC Lab
6	Pressure gauge	4	1800	500	3 old gauges taken from RAC Lab
7	Expansion Valve (Manual)	1	1500	500	-
8	Digital temperature controller	1	1200	1000	-
9	Control Valves	6	1000	2000	-
10	Energy meter	2	1000	-	Available in RAC Lab
11	Copper pipe	16.5m	850	1400	-
12	Refrigerant	1500gm	700	1200	-
13	Relay	1	2000	-	Available in RAC Lab
14	Temperature gauge	6	600	-	Available in RAC Lab
16	Main switch	1	500	500	-
17	Wiring	30m	500	500	-
18	Refrigerant charging line	1	500	300	-
19	Stainless Steel Drum	1	500	-	Available in RAC Lab
20	Flare nut	15	400	600	-
21	Condenser	1	400	500	-
22	Heater	1	300	300	-
23	Tee fitting	15	300	300	-
24	Ampere meter	1	200	-	Available in RAC Lab
25	Insulation	-	200	200	-
26	Acetylene gas Cylinder	2	200	200	-
27	Voltmeter	1	200	100	-
28	Soldering material	-	150	100	-
29	Nitrogen gas	1	150	150	-
31	Nut and Bolt	-	150	200	-
33	Filter	1	50	50	-
34	Welding rods	5	100	100	-
34	Miscellaneous	-	3000	2500	-
TOTAL			**33950**	**26250**	

Table 1 – Details of cost analysis

Flow Rate (LPH)	Evaporator load temperature (^oC)	COP		
		Pure R134a	R134a + 0.5% Al_2O_3	R134a + 1% Al_2O_3
6.5	15-17	0.982	1.065	0.929
6.5	30-31	0.931	1.011	0.889
11	15-17	0.773	0.883	0.737
11	30-31	0.853	0.937	0.866

Table 2 – Average COP at 21^{o}C ± 1^{o}C ambient temperature

Flow Rate (LPH)	Evaporator load temperature (^oC)	Pure R134a						
		T_1 (^oC)	T_2 (^oC)	Condenser temperature drop (^oC)	T_3 (^oC)	T_4 (^oC)	Evaporator temperature gain (^oC)	T_{atm}
6.5	15-17	71.12	41.25	29.87	-4.54	15.09	19.63	21.51
6.5	30-31	71.62	37.46	34.16	-9.30	26.76	36.06	21.22
11	15-17	70.38	41.20	29.18	-3.45	15.24	18.69	21.92
11	30-31	74.92	41.02	33.90	-1.91	27.34	29.25	22.05

Table 3 – Average temperatures at all salient points, condenser temperature drop and evaporator temperature gain at 21^{o}C ± 1^{o}C for pure R134a

Flow Rate (LPH)	Evaporator load temperature (^oC)	R134a + 0.5% Al_2O_3						
		T_1 (^oC)	T_2 (^oC)	Condenser temperature drop (^oC)	T_3 (^oC)	T_4 (^oC)	Evaporator temperature gain (^oC)	T_{atm}
6.5	15-17	71.05	40.03	31.02	-6.84	17.03	23.87	21.25
6.5	30-31	71.50	35.74	35.75	-9.32	28.43	37.75	21.45
11	15-17	71.68	40.18	31.50	-3.32	16.95	20.27	21.98
11	30-31	74.08	39.13	34.95	-3.03	27.93	30.96	21.40

Table 4 – Average temperatures at all salient points, condenser temperature drop and evaporator temperature gain at 21^{o}C ± 1^{o}C for R134a + 0.5% Al_2O_3

Flow Rate (LPH)	Evaporator load temperature (^oC)	R134a + 1% Al_2O_3						
		T_1 (^oC)	T_2 (^oC)	Condenser temperature drop (^oC)	T_3 (^oC)	T_4 (^oC)	Evaporator temperature gain (^oC)	T_{atm}
6.5	15-17	71.37	36.13	35.23	-9.83	17.23	27.06	22.00
6.5	30-31	72.41	33.03	39.38	-10.59	28.97	39.56	22.32
11	15-17	73.12	37.00	36.12	-5.76	17.27	23.03	22.26
11	30-31	73.03	35.08	37.95	-7.21	28.16	35.37	21.87

Table 5 – Average temperatures at all salient points, condenser temperature drop and evaporator temperature gain at 21^{o}C ± 1^{o}C for R134a + 1% Al_2O_3

Flow Rate (LPH)	Evaporator load temperature (^oC)	COP		
		Pure R134a	R134a + 0.5% Al_2O_3	R134a + 1% Al_2O_3
6.5	15-17	0.855	0.935	0.780
6.5	30-31	0.909	0.975	0.861
11	15-17	0.658	0.766	0.615
11	30-31	0.802	0.897	0.839

Table 6 – Average COP at 28^{o}C ± 1^{o}C ambient temperature

Flow Rate (LPH)	Evaporator load temperature (^oC)	Pure R134a						
		T_1 (^oC)	T_2 (^oC)	Condenser temperature drop (^oC)	T_3 (^oC)	T_4 (^oC)	Evaporator temperature gain (^oC)	T_{atm}
6.5	15-17	73.11	44.22	28.89	-3.79	15.13	18.93	27.53
6.5	30-31	75.69	42.16	33.53	-9.11	26.30	35.41	27.28
11	15-17	72.31	43.44	28.87	-2.21	15.69	17.90	26.98
11	30-31	78.10	44.74	33.35	-1.19	27.48	28.68	28.69

Table 7 – Average temperatures at all salient points, condenser temperature drop and evaporator temperature gain at 28^{o}C ± 1^{o}C for pure R134a

Flow Rate (LPH)	Evaporator load temperature (^oC)	R134a + 0.5% Al_2O_3						
		T_1 (^oC)	T_2 (^oC)	Condenser temperature drop (^oC)	T_3 (^oC)	T_4 (^oC)	Evaporator temperature gain (^oC)	T_{atm}
6.5	15-17	74.03	43.83	30.21	-5.63	17.06	22.69	27.50
6.5	30-31	75.69	40.78	34.91	-8.89	28.18	37.08	27.32
11	15-17	73.84	44.11	29.74	-2.79	17.08	19.87	28.00
11	30-31	80.73	46.33	34.40	-2.38	27.68	30.05	27.26

Table 8 – Average temperatures at all salient points, condenser temperature drop and evaporator temperature gain at $28^oC \pm 1^oC$ for R134a + 0.5% Al_2O_3

Flow Rate (LPH)	Evaporator load temperature (^oC)	R134a + 1% Al_2O_3						
		T_1 (^oC)	T_2 (^oC)	Condenser temperature drop (^oC)	T_3 (^oC)	T_4 (^oC)	Evaporator temperature gain (^oC)	T_{atm}
6.5	15-17	72.23	38.05	34.18	-8.50	17.86	26.36	28.21
6.5	30-31	78.65	39.77	38.88	-9.46	28.42	37.88	28.38
11	15-17	77.21	41.25	35.96	-4.92	17.33	22.25	28.53
11	30-31	76.94	39.53	37.41	-6.41	27.88	34.29	27.57

Table 9 – Average temperatures at all salient points, condenser temperature drop and evaporator temperature gain at $28^oC \pm 1^o$ for R134a + 1% Al_2O_3